

Table 1 Clinical characteristics

Variables	Total (n = 138)	With SEC (n = 21)	Without SEC (n = 117)	P-value
Age, years	63 ± 10	66 ± 9	63 ± 11	0.16
Male, n (%)	99 (72)	14 (67)	85 (73)	0.31
Body mass index, kg/m ²	23.5 ± 3.0	24.3 ± 3.5	23.4 ± 2.9	0.24
Heart rate, bpm	65 ± 12	66 ± 14	64 ± 11	0.62
Atrial fibrillation period, years	3.0 ± 3.5	2.6 ± 2.8	3.1 ± 3.6	0.53
Hypertension, n (%)	79 (57)	15 (71)	64 (55)	0.15
Diabetes mellitus, n (%)	22 (16)	5 (24)	17 (15)	0.28
Heart failure, n (%)	20 (14)	7 (33)	13 (11)	0.008
History of thromboembolism, n (%)	8 (6)	3 (14)	5 (4)	0.27
CHA2DS2-VASc score	2.1 ± 1.4	3.0 ± 1.6	1.9 ± 1.3	0.001
Anticoagulation therapy, n (%)	72 (52)	11 (52)	61 (52)	0.92
Haematocrit, %	35.3 ± 3.6	35.5 ± 3.0	35.2 ± 3.7	0.78
International normalized ratio of prothrombin time ^a	1.9 ± 0.5	2.0 ± 0.4	1.9 ± 0.5	0.70
Left atrial volume by computed tomography, cm ³	74 ± 19	87 ± 22	71 ± 18	0.0003
Left atrial volume index by computed tomography, cm ³ /m ²	58 ± 17	69 ± 24	56 ± 15	0.001

SEC, spontaneous echo contrast.

^aInternational normalized ratio of prothrombin time was an average value in patients receiving warfarin.

Table 2 Echocardiographic parameters

Variables	Total (n = 138)	With SEC (n = 21)	Without SEC (n = 117)	P-value
Transthoracic echocardiography				
Left ventricular ejection fraction, %	67 ± 9	65 ± 12	67 ± 8	0.26
Left ventricular mass index, g/m ^{1.7}	89 ± 27	109 ± 28	85 ± 26	0.0005
Diastolic early transmitral flow velocity (E), cm/s	60.4 ± 19.5	64.4 ± 31.8	59.6 ± 16.5	0.31
Diastolic early mitral annular velocity (e'), cm/s	6.9 ± 2.5	5.5 ± 2.7	7.1 ± 2.4	0.007
Diastolic late transmitral flow velocity (A), cm/s	64.5 ± 18.3	63.3 ± 14.2	64.8 ± 19.0	0.75
Diastolic late mitral annular velocity (a'), cm/s	8.1 ± 2.4	5.9 ± 1.9	8.5 ± 2.2	<0.0001
Diastolic early transmitral flow velocity/late transmitral flow velocity (E/A)	0.99 ± 0.42	0.90 ± 0.32	1.00 ± 0.43	0.32
Diastolic early transmitral flow velocity/mitral annular velocity (E/e')	10.7 ± 4.9	13.5 ± 8.5	10.2 ± 3.8	0.004
Class of diastolic dysfunction ^a				
Normal function, n (%)	23 (17)	2 (10)	21 (18)	0.53
Grade I (impaired relaxation), n (%)	27 (20)	5 (24)	22 (19)	
Grade II (pseudo normal left ventricular filling), n (%)	53 (38)	6 (29)	47 (40)	0.34
Grade III (restrictive filling), n (%)	35 (25)	8 (38)	27 (23)	
Transoesophageal echocardiography				
Left-atrial appendage flow velocity, cm/s	49.4 ± 16.5	32.2 ± 11.1	52.5 ± 15.4	<0.0001

SEC, spontaneous echo contrast.

^aClass of diastolic dysfunction recommended by the American Society of Echocardiography and the European Association of Echocardiography.

Association with a' and surrogate makers for LA thrombus

We divided the study patients into four groups based on the quartile of a', and compared the incidence of SEC and LA appendage flow velocity among the quartiles. As demonstrated in Figure 1,

more patients in the lowest quartile of a' (≤6.4 cm/s) had SEC than those in the other quartiles (44 vs. 6%, P < 0.0001). Figure 2 shows that patients in the lowest quartile of a' had significantly lower LA appendage flow velocity than those in the other quartiles (39 ± 13 vs. 53 ± 16 cm/s, P < 0.0001). Furthermore,

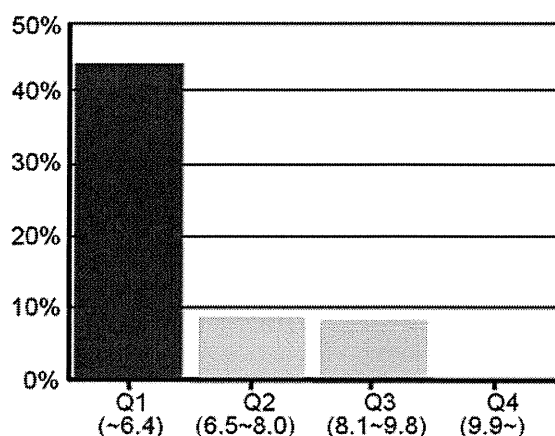


Figure 1 Incidence of spontaneous echo contrast in each quartile (Q) of diastolic late mitral annular velocity (a'). Range of a' in each quartile is expressed in parentheses. More patients in the lowest quartile of a' (Q1) had spontaneous echo contrast than those in the other quartiles (Q2–Q4, $P < 0.0001$).

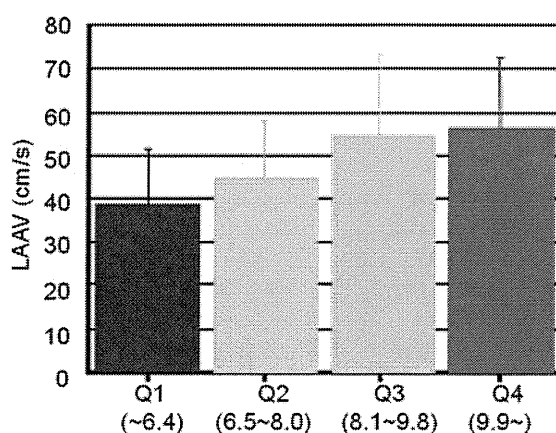


Figure 2 Left atrial appendage flow velocity (LAAV) in each quartile (Q) of diastolic late mitral annular velocity (a'). Range of a' in each quartile is expressed in parentheses. Patients in the lowest quartile of a' (Q1) had significantly lower LAAV than those in the other quartiles (Q2–Q4, $P < 0.0001$). Increased quartile of a' was significantly associated with higher LAAV ($P < 0.0001$ by analysis of variance).

increased quartile of a' was significantly associated with higher LA appendage flow velocity ($P < 0.0001$ by analysis of variance).

Receiver-operating characteristic curve analysis was performed to determine the best cut-off value of a' for the prediction of SEC (area under the curve = 0.82, 95% CI = 0.74–0.91) as shown in Figure 3. The best cut-off value of a' was 7.0 cm/s with a sensitivity of 80%, specificity of 81%, and predictive accuracy of 80%.

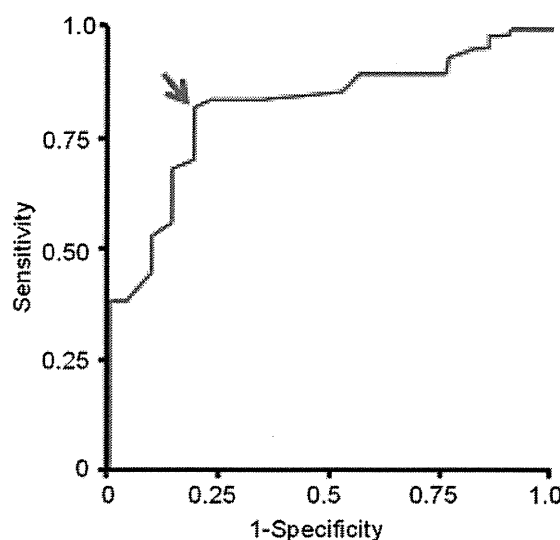


Figure 3 Receiver-operating characteristics curve for the prediction of spontaneous echo contrast. The area under the curve was 0.82, and the 95% CI was 0.74–0.91. A red arrow indicates the optimal cut-off point.

Transthoracic echocardiographic factors associated with SEC

In order to determine the echocardiographic factors associated with SEC, we performed univariate and multivariate logistic regression analyses (Table 3). In the univariate analysis, high CHA2DS2-VASc score, large LA volume index by computed tomography, increased LV mass index, increased E/e' , decreased a' were the associated factors. As a result of multivariate analysis, increased CHA2DS2-VASc score and decreased a' were independently associated with SEC.

The value of a' and history of thromboembolism

Of the 138 patients, eight (6%) patients had a history of thromboembolism. The value of a' was significantly lower in patients with than without a history of thromboembolism (6.3 ± 2.9 vs. 8.2 ± 2.3 cm/s, $P = 0.03$). In addition, the frequency of patients with a history of thromboembolism tended to be higher in the lowest quartile of a' compared with the other quartiles (12 vs. 4%, $P = 0.10$).

LA pump function and left ventricular filling pressure: association with LA volume

We investigated the relationship between a' and E/e' which represents left ventricular filling pressure. Seventeen of 138 (12%) patients in our study had $E/e' > 15$, which is thought to be associated with elevated left ventricular filling pressure.¹⁸ E/e' showed a significant inverse correlation with a' ($r = -0.43$, $P < 0.0001$). Furthermore, patients with $E/e' > 15$ had significantly

Table 3 Univariate and multivariate models of factors associated with spontaneous echo contrast

Variables	Univariate			Multivariate		
	OR	95% CI	P-value	OR	95% CI	P-value
Age	1.04	0.99–1.09	0.16	—	—	—
Male	0.75	0.28–2.04	0.58	—	—	—
Body mass index	1.003	0.99–1.01	0.51	—	—	—
CHA2DS2-VASc score	2.43	1.45–4.10	0.0008	2.32	1.06–4.97	0.03
Left-atrial volume index by computed tomography	1.10	1.03–1.19	0.007	1.08	0.98–1.15	0.12
Left ventricular mass index	1.04	1.02–1.06	0.002	1.01	0.98–1.03	0.75
Left ventricular ejection fraction	0.97	0.93–1.02	0.26	—	—	—
Diastolic early transmitral flow velocity/mitral annular velocity (E/e')	1.12	1.02–1.21	0.01	0.92	0.77–1.09	0.26
Diastolic late mitral annular velocity (a'), cm/s	0.61	0.49–0.77	<0.0001	0.61	0.42–0.84	0.0026

lower a' than those with $E/e' \leq 15$ (6.2 ± 2.3 vs. 8.3 ± 2.3 cm/s, $P = 0.0004$).

On the other hand, a' negatively correlated with pre-atrial contraction LA volume and LA volume index ($r = -0.41$, $P < 0.0001$ and $r = -0.37$, $P < 0.0001$), and E/e' positively correlated with LA volume and LA volume index ($r = 0.41$, $P < 0.0001$ and $r = 0.41$, $P < 0.0001$).

Discussion

The major findings of this study are as follows. Decreased a' was significantly associated with SEC and reduced LA appendage flow velocity. Furthermore, multivariate analysis revealed that decreased a' was independently associated with SEC. The optimal cut-off value of a' for predicting SEC was 7.0 cm/s.

Recently, Tamura *et al.*¹⁹ reported a different transthoracic echocardiographic method to estimate the risk of ischaemic stroke in patients with atrial fibrillation. They showed that decreased LA appendage wall velocity measured by transthoracic echocardiography was associated with increased risk of cerebrovascular events. The advantage of our method is that a' would be more easily measured than LA appendage wall velocity in most cases. In 9.4% of patients, according to their report, LA appendage wall velocity could not be measured; while a' could not be measured only in one of 180 (0.6%) patients in this study.

Previous studies reported that in patients with paroxysmal atrial fibrillation, irrespective of cardiac rhythm during transoesophageal echocardiography, SEC in the LA was significantly associated with an increased risk of thromboembolic events.^{2,3} In addition, patients with low LA appendage flow during atrial fibrillation were shown to have increased risk of thrombus formation.⁴ Handke *et al.*⁵ demonstrated that, independent of cardiac rhythm, low LA appendage flow was closely related to SEC and thrombus formation.

A possible explanation for the relationship between decreased a' and LA blood stasis is as follows. The impairment of LA contractile function during atrial fibrillation and atrial stunning would be more severe in patients with advanced atrial remodelling.¹² Decreased a' was also reported to reflect advanced atrial

remodelling in patients with paroxysmal atrial fibrillation.⁸ Therefore, decreased a' could indicate LA low blood flow.

The contraction of atrial myocardium is proportional to its initial length, according to the Frank–Starling mechanism.^{20,21} Therefore, LA pump function should be enhanced in response to larger pre-atrial contraction LA volume (preload) to some extent. However, there was an inverse correlation between LA pump function (a') and pre-atrial contraction LA volume in the present study. The Frank–Starling curve has been shown to have a descending limb at very large atrial volumes, as demonstrated by Anwar *et al.*¹⁷ It is possible that patients in this study were operating on the descending limb of the Frank–Starling curve, and this may explain the inverse correlation between LA pump function and pre-atrial contraction LA volume. In addition, depressed LA myocardial contractility due to further progression of LA structural remodelling beyond the range of compensation could explain this inverse correlation. A previous study showed that LA pump function was inversely correlated with LA volume (preload) in patients with paroxysmal atrial fibrillation.⁸

Decreased a' could be used as a substitute for SEC and reduced LA appendage flow velocity. Measurement of a' using transthoracic echocardiography is easy and may provide additional information about the risk of LA thrombus formation. However, this study included a selected and limited number of patients, and an association between decreased a' and thromboembolic events remains uncertain. Further studies are required before this method is used to manage patients in routine clinical practice.

This study has several limitations. First, we mainly investigated the relationship between a' and surrogate makers for LA thrombus formation (SEC and appendage flow velocity), and could not directly assess the relationship between a' and LA thrombus, because the number of patients with LA thrombus was too small for adequate statistical analysis. However, the relationship between SEC or LA appendage flow velocity during sinus rhythm and stroke risk in patients with paroxysmal atrial fibrillation has never been fully determined. Next, recent episodes of atrial fibrillation might cause subsequent atrial stunning, and was possible to influence echocardiographic data. To avoid this influence, we excluded patients that had symptomatic episodes of atrial

fibrillation within 2 days prior to echocardiography. However, atrial stunning could last longer than 2 days, and we might fail to recognize atrial fibrillation events without significant symptom. Additionally, the grade of SEC was not evaluated in this study, although the prevalence of LA thrombus in atrial fibrillation is associated with a higher grade of SEC.⁷ Furthermore, we used same patients to determine the best cut-off value of a' for the prediction of SEC and to evaluate the diagnostic performance of the determined cut-off value, which is not necessarily a fair method to test diagnostic performance. Finally, there are some technical difficulties with Doppler echocardiography. The motion of the mitral annulus is not entirely due to myocardial contraction, but rather is the summation of contraction, rotation, and translation of the heart. Furthermore, a' is dependent on the Doppler angle and can change slightly from beat to beat.

In conclusion, decreased a' during sinus rhythm may be a useful parameter for the prediction of LA blood stasis in patients with non-valvular paroxysmal atrial fibrillation.

Acknowledgements

The authors thank Maya Nakagawa, medical sonographer for her support in data collection.

Conflict of interest: none declared.

References

1. Camm AJ, Lip GY, De Caterina R, Savelieva I, Atar D, Hohloser SH et al. 2012 focused update of the ESC Guidelines for the management of atrial fibrillation. *Eur Heart J* 2012;**33**:2719–47.
2. Castello R, Pearson AC, Labovitz AJ. Prevalence and clinical implications of atrial spontaneous contrast in patients undergoing transesophageal echocardiography. *Am J Cardiol* 1990;**65**:1149–53.
3. Chimowitz MI, DeGeorgia MA, Poole RM, Hepner A, Armstrong WM. Left atrial spontaneous echo contrast is highly associated with previous stroke in patients with atrial fibrillation or mitral stenosis. *Stroke* 1993;**24**:1015–9.
4. Mugge A, Kuhn H, Nikutta P, Grote J, Lopez JA, Daniel WG. Assessment of left atrial appendage function by biplane transesophageal echocardiography in patients with nonrheumatic atrial fibrillation: identification of a subgroup of patients at increased embolic risk. *J Am Coll Cardiol* 1994;**23**:599–607.
5. Handke M, Harloff A, Hetzel A, Olschewski M, Bode C, Geibel A. Left atrial appendage flow velocity as a quantitative surrogate parameter for thromboembolic risk: determinants and relationship to spontaneous echocontrast and thrombus formation—a transesophageal echocardiographic study in 500 patients with cerebral ischemia. *J Am Soc Echocardiogr* 2005;**18**:1366–72.
6. Asinger RW, Koehler J, Pearce LA, Zabalgoitia M, Blackshear JL, Fenster PE et al. Pathophysiologic correlates of thromboembolism in nonvalvular atrial fibrillation: II. Dense spontaneous echocardiographic contrast (The Stroke Prevention in Atrial Fibrillation [SPAF-III] study). *J Am Soc Echocardiogr* 1999;**12**:1088–96.
7. Fatkin D, Kelly RP, Feneley MP. Relations between left atrial appendage blood flow velocity, spontaneous echocardiographic contrast and thromboembolic risk in vivo. *J Am Coll Cardiol* 1994;**23**:961–9.
8. Toh N, Kanzaki H, Nakatani S, Ohara T, Kim J, Kusano KF et al. Left atrial volume combined with atrial pump function identifies hypertensive patients with a history of paroxysmal atrial fibrillation. *Hypertension* 2010;**55**:1150–6.
9. Nagueh SF, Sun H, Kopelen HA, Middleton KJ, Khoury DS. Hemodynamic determinants of the mitral annulus diastolic velocities by tissue Doppler. *J Am Coll Cardiol* 2001;**37**:278–85.
10. Thomas L, Levett K, Boyd A, Leung DY, Schiller NB, Ross DL. Changes in regional left atrial function with aging: evaluation by Doppler tissue imaging. *Eur J Echocardiogr* 2003;**4**:92–100.
11. Khankirawatana B, Khankirawatana S, Peterson B, Mahrous H, Porter TR. Peak atrial systolic mitral annular velocity by Doppler tissue reliably predicts left atrial systolic function. *J Am Soc Echocardiogr* 2004;**17**:353–60.
12. Khan IA. Atrial stunning: determinants and cellular mechanisms. *Am Heart J* 2003;**145**:787–94.
13. Manning WJ, Weintraub RM, Waksmonski CA, Haering JM, Rooney PS, Maslow AD et al. Accuracy of transesophageal echocardiography for identifying left atrial thrombi. A prospective, intraoperative study. *Ann Intern Med* 1995;**123**:817–22.
14. Seward JB, Khandheria BK, Oh JK, Freeman WK, Tajik AJ. Critical appraisal of transesophageal echocardiography: limitation, pitfalls, and complications. *J Am Soc Echocardiogr* 1992;**5**:288–305.
15. Lang RM, Bierig M, Devereux RB, Flachskampf FA, Foster E, Pellikka PA et al. Recommendations for chamber quantification: a report from the American Society of Echocardiography's Guidelines and Standards Committee and the Chamber Quantification Writing Group, developed in conjunction with the European Association of Echocardiography, a branch of the European Society of Cardiology. *J Am Soc Echocardiogr* 2005;**18**:1440–63.
16. Chirinos JA, Segers P, De Buyzere ML, Kronmal RA, Raja MW, De Bacquer D et al. Left ventricular mass: allometric scaling, normative values, effect of obesity, and prognostic performance. *Hypertension* 2010;**56**:91–8.
17. Nagueh SF, Appleton CP, Gillebert TC, Marino PN, Oh JK, Smiseth OA et al. Recommendations for the evaluation of left ventricular diastolic function by echocardiography. *Eur J Echocardiogr* 2009;**10**:165–93.
18. Ommen SR, Nishimura RA, Appleton CP, Miller FA, Oh JK, Redfield MM et al. Clinical utility of Doppler echocardiography and tissue Doppler imaging in the estimation of left ventricular filling pressures: a comparative simultaneous Doppler-catheterization study. *Circulation* 2000;**102**:1788–94.
19. Tamura H, Watanabe T, Nishiyama S, Sasaki S, Wanezaki M, Arimoto T et al. Prognostic value of low left atrial appendage wall velocity in patients with ischemic stroke and atrial fibrillation. *J Am Soc Echocardiogr* 2012;**25**:576–83.
20. Anwar AM, Geleijnse ML, Soliman OI, Nemes A, ten Cate FJ. Left atrial Frank-Starling law assessed by real-time, three-dimensional echocardiographic left atrial volume changes. *Heart* 2007;**93**:1393–7.
21. Stefanadis C, Dernellis J, Toutouzas P. A clinical appraisal of left atrial function. *Eur Heart J* 2001;**22**:22–36.

Complement C1q Activates Canonical Wnt Signaling and Promotes Aging-Related Phenotypes

Atsuhiko T. Naito,^{1,3} Tomokazu Sumida,⁴ Seitaro Nomura,⁴ Mei-Lan Liu,⁴ Tomoaki Higo,¹ Akito Nakagawa,¹ Katsuki Okada,¹ Taku Sakai,¹ Akihito Hashimoto,¹ Yurina Hara,¹ Ippei Shimizu,⁴ Weidong Zhu,⁴ Haruhiro Toko,⁴ Akemi Katada,⁴ Hiroshi Akazawa,^{1,3} Toru Oka,^{1,3} Jong-Kook Lee,^{1,3} Tohru Minamino,⁴ Toshio Nagai,⁴ Kenneth Walsh,⁵ Akira Kikuchi,² Misako Matsumoto,⁶ Marina Botto,⁷ Ichiro Shiojima,^{1,3} and Issei Komuro^{1,3,4,*}

¹Department of Cardiovascular Medicine

²Department of Molecular Biology and Biochemistry

Osaka University Graduate School of Medicine, Osaka 565-0871, Japan

³Japan Science and Technology Agency, CREST, Tokyo 102-0075, Japan

⁴Department of Cardiovascular Science and Medicine, Chiba University Graduate School of Medicine, Chiba 260-8670, Japan

⁵Molecular Cardiology, Whitaker Cardiovascular Institute, Boston University School of Medicine, Boston, MA 02118, USA

⁶Department of Microbiology and Immunology, Graduate School of Medicine, Hokkaido University, Hokkaido 060-8638, Japan

⁷Centre for Complement and Inflammation Research, Department of Medicine, Imperial College London, London SW7 2AZ, UK

*Correspondence: komuro-tky@umin.ac.jp

DOI 10.1016/j.cell.2012.03.047

SUMMARY

Wnt signaling plays critical roles in development of various organs and pathogenesis of many diseases, and augmented Wnt signaling has recently been implicated in mammalian aging and aging-related phenotypes. We here report that complement C1q activates canonical Wnt signaling and promotes aging-associated decline in tissue regeneration. Serum C1q concentration is increased with aging, and Wnt signaling activity is augmented during aging in the serum and in multiple tissues of wild-type mice, but not in those of C1qa-deficient mice. C1q activates canonical Wnt signaling by binding to Frizzled receptors and subsequently inducing C1s-dependent cleavage of the ectodomain of Wnt coreceptor low-density lipoprotein receptor-related protein 6. Skeletal muscle regeneration in young mice is inhibited by exogenous C1q treatment, whereas aging-associated impairment of muscle regeneration is restored by C1s inhibition or C1qa gene disruption. Our findings therefore suggest the unexpected role of complement C1q in Wnt signal transduction and modulation of mammalian aging.

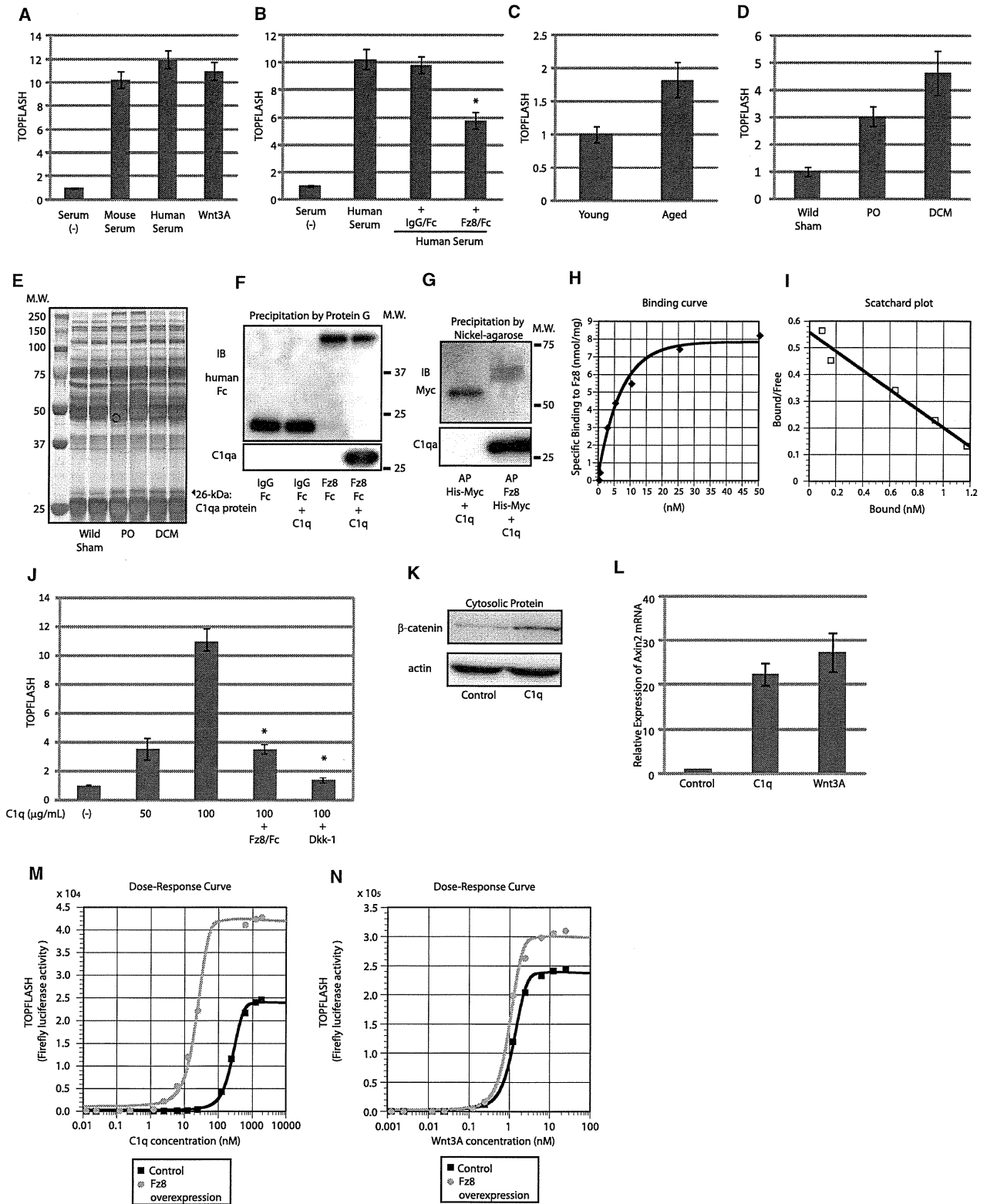
INTRODUCTION

Wnts constitute a large family of secreted proteins that elicit evolutionarily conserved intracellular signaling and affect diverse cellular responses during development. Wnt signaling also plays critical roles in various physiological and pathological processes in adult organisms, including stem cell self-renewal/differentia-

tion, degenerative diseases, and carcinogenesis (Blanpain et al., 2007; Clevers, 2006; Logan and Nusse, 2004). The β -catenin-dependent canonical Wnt pathway is the most understood signaling cascade initiated by Wnt proteins. Upon Wnt stimulation, cytosolic β -catenin is stabilized and translocates to the nucleus, where it binds to T cell factor/Lymphoid enhancer factor (Tcf/Lef) and induces Tcf/Lef-dependent transcription (Logan and Nusse, 2004). This canonical Wnt signaling is mediated by two types of cell surface receptors, the Frizzled (Fz) family of serpentine proteins and the single-transmembrane protein low-density lipoprotein receptor-related protein 5/6 (LRP5/6) (Angers and Moon, 2009; MacDonald et al., 2009).

Recent studies have revealed a role of Wnt signaling in the regulation of mammalian aging. Wnt/ β -catenin signaling is augmented in a mouse model of accelerated aging (Liu et al., 2007), and inhibition of canonical Wnt signaling reverses the aging-associated impairment of skeletal muscle regeneration (Brack et al., 2007). Moreover, this age-related activation of Wnt signaling was attributed to the substance(s) in the serum that binds to the extracellular cysteine-rich domain (CRD) of Fz (Brack et al., 2007). However, because Wnt proteins tightly bind to the cell surface and/or extracellular matrix and are thought to act in a short-range manner (Kikuchi et al., 2007; White et al., 2007), the substance(s) in the serum that activates Wnt signaling was assumed to be distinct from classical Wnt proteins.

Here, we show that complement C1q is an activator of Wnt signaling. C1q activates canonical Wnt signaling by binding to Fz receptors and subsequently inducing C1s-dependent cleavage of the ectodomain of LRP6. Serum C1q concentration and the expression of C1q in various tissues are increased with aging, which are associated with increased Wnt signaling activity in serum and in multiple tissues during aging. We further demonstrate that activation of Wnt signaling by C1q accounts for the



impaired regenerative capacity of skeletal muscle in aged mice. These results suggest that C1q activates Wnt signaling and modulates mammalian aging-related phenotypes.

RESULTS

Complement C1q Is a Fz-Binding Protein in the Serum

Consistent with a previous report (Brack et al., 2007), mouse and human serum activated canonical Wnt signaling, as assessed by the TOPFLASH reporter gene assay that reflects Tcf/Lef-dependent transcription (Figure 1A). Human serum-induced activation of Wnt signaling was partly suppressed by a Fz8 CRD-IgG/Fc fusion protein (Fz8/Fc), but not by IgG/Fc (Figure 1B), and serum from aged mice showed higher TOPFLASH activity than serum from young mice (Figure 1C). We also found that the serum obtained from two different mouse models of heart failure more potently increased TOPFLASH activity compared with serum from aged mice (Figure 1D). We therefore hypothesized that the serum of mice with heart failure contains the Wnt activator more abundantly than that of aged mice, and we used the former as a starting material to isolate the Wnt activator in the serum. Precipitation of Fz8/Fc-binding proteins followed by SDS-PAGE identified a 26 kDa protein that was upregulated in the serum from mice with heart failure (Figure 1E). Mass spectrometric analysis revealed that this 26 kDa protein was complement C1qa, which is a major constituent of complement C1q.

C1q is composed of 18 polypeptides: 6 C1qa, 6 C1qb, and 6 C1qc chains, each encoded by 3 individual genes. Although C1q is known to bind to Fc portion of aggregated immunoglobulins, purified C1q was precipitated by Fz8/Fc and a Fz8 CRD-alkaline phosphatase (AP) fusion protein, but not by IgG/Fc or AP protein in a pull-down assay (Figures 1F and 1G and Figures S1A and S1B available online), indicating that C1q binds to CRD of Fz8. C1q also bound to CRD of other Fz receptors such as Fz1, 2, 4, and 7 (Figure S1C).

Complement C1q Is an Activator of Canonical Wnt Signaling

We next investigated whether C1q is a specific ligand for Fz receptors. A binding assay demonstrated that the interaction

between C1q and Fz8 CRD was specific and saturable (Figure 1H). A Scatchard plot analysis revealed that C1q has a single binding site for Fz8 CRD, with a binding affinity comparable to that of Wnt3A ($K_{d_{C1q}}$: 2.8 nM, $K_{d_{Wnt3A}}$: 1.25 nM) (Figures 1I, S1D, and S1E). A heterologous competition assay revealed that C1q and Wnt compete with each other for the binding to Fz8 CRD (Figure S1F). Purified C1q dose dependently increased TOPFLASH activity (Figure 1J), stabilized cytosolic β -catenin (Figure 1K), and increased the expression of *Axin2*, a well-established target gene of canonical Wnt signaling (Figure 1L). C1q-induced TOPFLASH activity was inhibited by Fz8/Fc or Dkk1 (Figure 1J). These results strongly suggest that C1q is a Fz-binding protein that activates canonical Wnt signaling.

Despite the similar binding affinity to Fz receptor, dose-response curves of C1q and Wnt3A on TOPFLASH activity revealed that the EC_{50} of C1q on activation of Wnt signaling (259 nM) was 200-fold higher than that of Wnt3A (1.27 nM) (Figures 1M and 1N). Based on the mode of C1q activation by immunoglobulins or SIGN-R1 (Duncan and Winter, 1988; Kang et al., 2006; Schumaker et al., 1986), in which the binding of multiple or aggregated immunoglobulins or SIGN-R1 to C1q initiates C1q activation, we hypothesized that increasing the amount of Fz receptors may promote C1q-induced activation of Wnt signaling. Indeed, overexpression of Fz8 decreased the EC_{50} of C1q by 13-fold (259 nM to 22.8 nM), whereas the EC_{50} of Wnt3A was less affected (1.27 nM to 0.852 nM) (Figures 1M and 1N). These results suggest that the mode of Wnt signaling activation by C1q is distinct from that by Wnt3A and is affected by the cellular context, including the density of Fz receptors.

C1q Mediates Serum-Induced Activation of Wnt Signaling In Vitro and Maintains Basal Wnt Signaling Activity in Multiple Tissues In Vivo

We assessed whether serum-induced activation of Wnt signaling is attributable to C1q. C1q-depleted serum or serum treated with Fz8/Fc showed lower TOPFLASH activity compared with normal serum and C3- or C5-depleted serum, and addition of Fz8/Fc to C1q-depleted serum did not further reduce TOPFLASH activity (Figure 2A). Likewise, serum from C1qa-deficient mice showed lower TOPFLASH activity compared with serum from wild-type

Figure 1. Complement C1q Binds to Fz and Activates Wnt Signaling

(A–D) TOPFLASH assay. Mouse and human serum (10%) and Wnt3A protein (10 ng/ml) activated canonical Wnt signaling to the same degree (A). Activation of Wnt signaling by human serum was suppressed by Fz8/Fc (500 ng/ml). * $p < 0.05$ versus human serum (B). Serum-induced Wnt signaling activity was higher in aged mice (C) and in mice with heart failure (D). Data are presented as mean \pm SD. PO, mice with pressure overload; DCM, mice with dilated cardiomyopathy. (E) Silver staining of SDS-PAGE gel. Serum obtained from control mice and mice with heart failure were incubated with Fz8/Fc and precipitated by protein G. SDS-PAGE of the precipitates revealed that the amount of a protein of ~26 kDa (arrowhead) was increased in the serum from mice with heart failure. PO, mice with pressure overload; DCM, mice with dilated cardiomyopathy. (F and G) Pull-down assay. C1q was precipitated by Fz8/Fc, but not by IgG/Fc (F). C1q was precipitated by Fz8 CRD-AP, but not by AP (G). (H and I) Binding kinetics of C1q to Fz8 CRD. A binding curve (H) and a Scatchard plot (I) are shown. (J) TOPFLASH assay. C1q dose dependently activated canonical Wnt signaling, which was blocked by Fz8/Fc (20 μ g/ml) or Dkk-1 (20 ng/ml). Data are presented as mean \pm SD. * $p < 0.01$ versus of C1q (100 μ g/ml). (K) β -catenin stabilization assay. β -catenin stabilization assay was performed in HEK293 cells 1 hr after C1q stimulation (200 μ g/ml). (L) *Axin2* mRNA levels. C1q (100 μ g/ml) and Wnt3A (10 ng/ml) activate canonical Wnt signaling to the same degree as assessed by *Axin2* mRNA induction in HEK293 cells. *Axin2* mRNA was assessed 24 hr after stimulation. Data are presented as mean \pm SD. (M and N) Dose-response curves of C1q and Wnt3A on TOPFLASH activity. Fz8 overexpression induced marked leftward shift of the response curve of C1q-induced TOPFLASH activity (M) but had minimal effects on that of Wnt3A-induced TOPFLASH activity (N). See also Figure S1.

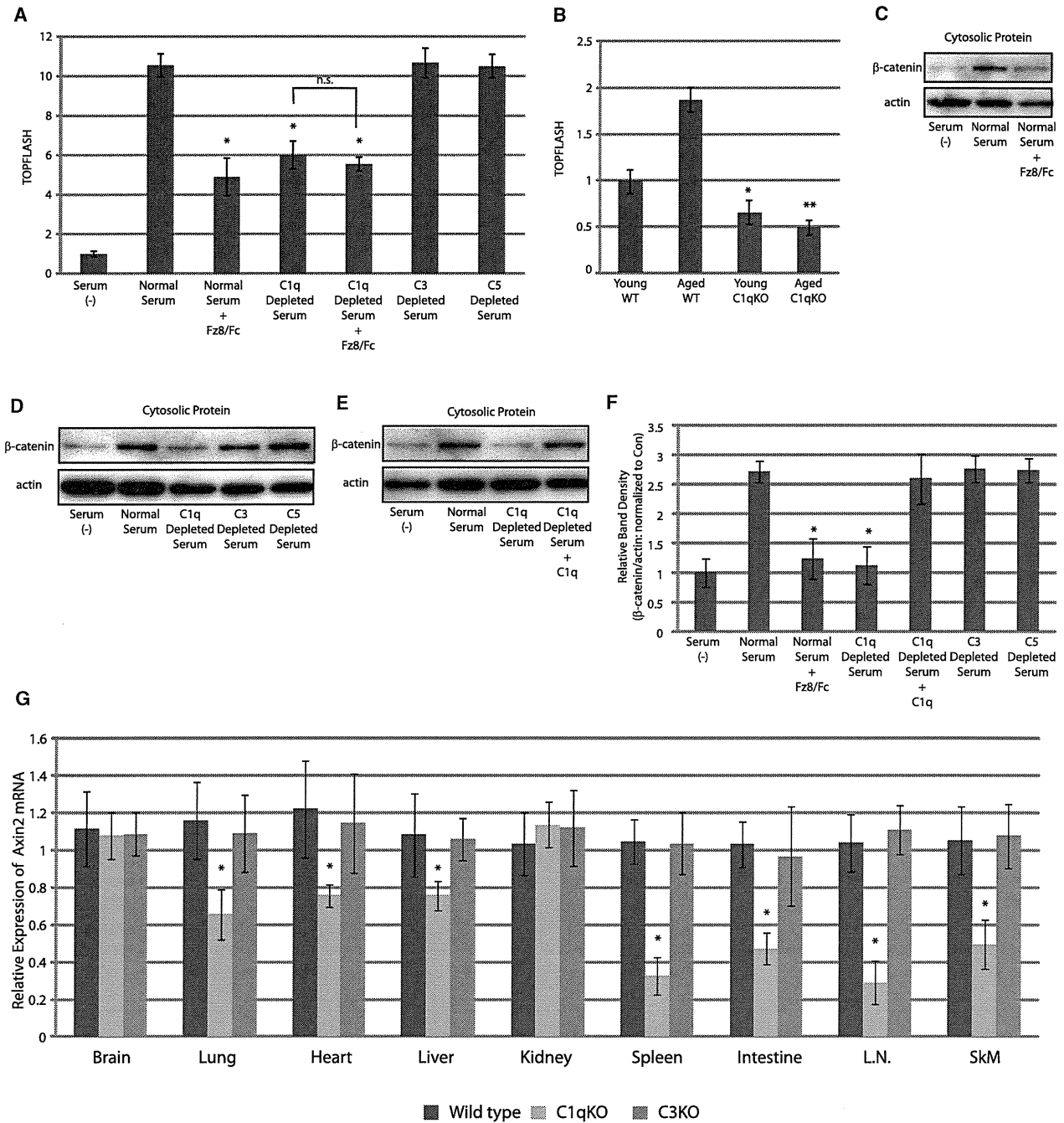


Figure 2. C1q Mediates Serum-Induced Activation of Wnt Signaling In Vitro and Is Required for Basal Wnt Signaling Activity In Vivo

(A) TOPFLASH assay. Wnt signaling activation by serum was partially blocked by Fz8/Fc (10 μg/ml) or C1q depletion, but not by C3 or C5 depletion. Combination of Fz8/Fc and C1q depletion did not further decrease TOPFLASH activity. Data are presented as mean ±SD. *p < 0.01 versus normal serum.

(B) TOPFLASH assay. In wild-type (WT) mice, serum from aged mice showed higher TOPFLASH activity than serum from young mice. Serum from young C1qa-deficient mice showed lower TOPFLASH activity compared with serum from young WT mice, and the elevation of TOPFLASH activity during aging was not observed in C1qa-deficient mice. Data are presented as mean ±SD. *p < 0.01 versus serum obtained from young WT mice. **p < 0.01 versus aged serum obtained from WT mice.

(C–F) β-catenin stabilization assay. Human serum activated Wnt signaling, which was abolished by Fz8/Fc (10 μg/ml) (C). Wnt signaling activation by serum was also abolished by C1q depletion, but not by C3 or C5 depletion (D). Reduced Wnt signaling activation by C1q depletion was fully restored by C1q (10 μg/ml) application (E). The results were quantified by measuring the relative amount of β-catenin over actin (F). Data are presented as mean ±SD. *p < 0.05 versus normal human serum (n = 5).

or C3-deficient mice at the age of 3 months (Figure S2). Moreover, augmentation of serum TOPFLASH activity by aging was not observed in C1qa-deficient mice (Figure 2B). Thus, C1q mediates serum-induced activation of Wnt signaling and accounts for increased Wnt signal activation by serum from aged mice.

We also assessed the activation of Wnt signaling by analyzing cytosolic β -catenin level at 1 hr after the treatment with serum because TOPFLASH assay is performed at relatively later time points after serum stimulation and therefore may be affected by other factors that indirectly modulate Tcf/Lef-dependent transcription. Indeed, unlike TOPFLASH assay, serum-induced activation of Wnt signaling as assessed by β -catenin stabilization was almost completely blunted by Fz8/Fc or C1q depletion, but not by C3 or C5 depletion, which was fully recovered by the addition of C1q (Figures 2C–2F). These results further support the notion that C1q is responsible for serum-induced activation of canonical Wnt signaling.

We further investigated whether activation of Wnt signaling by C1q is physiologically relevant in vivo. Real-time PCR analysis revealed that expression levels of *Axin2* gene were decreased in various tissues of C1qa-deficient mice, but not in those of C3-deficient mice, most notably in spleen, intestine, lymph nodes, and skeletal muscle (Figure 2G). This result suggests that basal activity of canonical Wnt signaling is at least in part dependent on C1q and underscores the physiological relevance of C1q-induced Wnt signaling activation in vivo.

C1q Mediates Augmented Wnt Signaling Activity Associated with Aging

We next examined whether C1q mediates augmented Wnt signaling activity during aging. ELISA and western blot analysis revealed that serum C1q concentration was increased with aging (Figures 3A and 3B). It was previously reported that cells of the monocyte/macrophage lineage are the major source of serum C1q (Petry et al., 2001). Indeed, expression levels of C1q in peritoneal macrophages were higher in 1-year-old and 2-year-old mice than in young mice (2-months-old) (Figure 3C), consistent with the observation that serum C1q levels were upregulated at these ages (Figures 3A and 3B). Expression levels of C1q were upregulated in various tissues of 2-year-old mice (Figure 3D), suggesting that upregulation of C1q in macrophages causes an initial increase in serum C1q levels and that C1q produced in other tissues at later stages may contribute to a further increase in serum C1q levels.

We also assessed whether C1q is responsible for age-associated augmentation of Wnt signaling activity. An age-associated increase in *Axin2* mRNA was observed in various tissues of wild-type mice. On the other hand, there was no significant difference in *Axin2* mRNA levels between young and aged C1qa-deficient mice in all tissues examined (Figure 3E). Thus, C1q is responsible for augmented Wnt signaling activity in multiple tissues of aged animals.

C1q Activates Canonical Wnt Signaling by Inducing C1s-Dependent Cleavage of the Extracellular Domain of LRP6

The complement system is one of the major components of the mammalian immune responses and plays a pivotal role in innate immunity (Walport, 2001). The classical complement pathway is triggered by C1, which is composed of C1q and two proenzymes, C1r and C1s. Conventionally, C1q binds to aggregated immunoglobulins, which leads to conformational change and subsequent activation of C1q (Duncan and Winter, 1988; Schumaker et al., 1986). Upon C1q activation, C1r undergoes autoactivation and, in turn, cleaves and activates C1s. C1s then cleaves C2 and C4 to instigate following activation steps of the complement system. We therefore tested whether C1r/C1s is involved in C1q-induced activation of Wnt signaling. Consistent with the observation that purified C1q activates Wnt signaling in a serum-free condition (where no exogenous C1r/C1s is thought to exist) (Figures 1J–1L), western blot analysis revealed that both C1r and C1s are expressed in the target cells and secreted into the culture media (Figure 4A). Knockdown of C1r/C1s by siRNAs totally blunted C1q-induced cytosolic β -catenin stabilization and TOPFLASH activation (Figures 4B and 4C). Likewise, addition of C1 inhibitor (C1-INH), an endogenous inhibitor of C1r and C1s, or a neutralizing antibody against C1s (M241) (Matsumoto and Nagaki, 1986) strongly inhibited C1q-induced activation of Wnt signaling (Figure 4D). To test whether C1s is activated upon C1q-Fz interaction, we treated NIH 3T3 cells with C1q and C4 in a serum-free condition. C4 is a target of C1s, and its cleaved product, C4b, covalently binds to the cellular surface after cleavage. We found that overexpression of Fz8 pronouncedly enhanced C4b deposition on the cellular surface (Figures 4E and 4F). These results suggest that endogenous C1r and C1s are activated upon C1q-Fz binding and that C1q-induced activation of Wnt signaling requires protease activity of C1s.

In addition to C2 and C4, C1s has been reported to cleave other cell surface proteins such as major histocompatibility complex (MHC) class I molecules (Eriksson and Nissen, 1990). Because deletion of the extracellular domain of LRP6 results in constitutive activation of canonical Wnt signaling (Liu et al., 2003; Mao et al., 2001), we tested whether LRP6 is the target of C1s. Treatment of LRP6 extracellular domain-IgG/Fc fusion protein with active C1s resulted in the appearance of two major cleaved products (Figure 4G), and N-terminal amino acid sequencing revealed that LRP6 was cleaved between Arg792 and Ala793 in the third β -propeller domain. The C1s cleavage site of LRP6 was conserved in various species, and similar sequences were also found in the third β -propeller domain of LRP5 (Figure 4H). The C1s cleavage site of LRP6 is adjacent to the Dkk1-binding site (Ahn et al., 2011; Chen et al., 2011). However, the inhibitory effect of Dkk1 on C1q-induced Wnt activation (Figure 1J) does not appear to be due to the direct inhibition of LRP6 cleavage because Dkk-1 did not have major impact on in vitro cleavage of LRP6 by C1s (data not shown).

(G) Expression levels of *Axin2* mRNA in various tissues of 3-month-old wild-type (n = 8), C1qa-deficient (n = 8), and C3-deficient (n = 4) mice. Expression levels of *Axin2* gene expression were lower in various tissues of C1qa-deficient mice, but not in those of C3-deficient mice. Data are presented as mean \pm SD. *p < 0.05 compared with wild-type mice. L.N., lymph node; SkM, skeletal muscle. See also Figure S2.

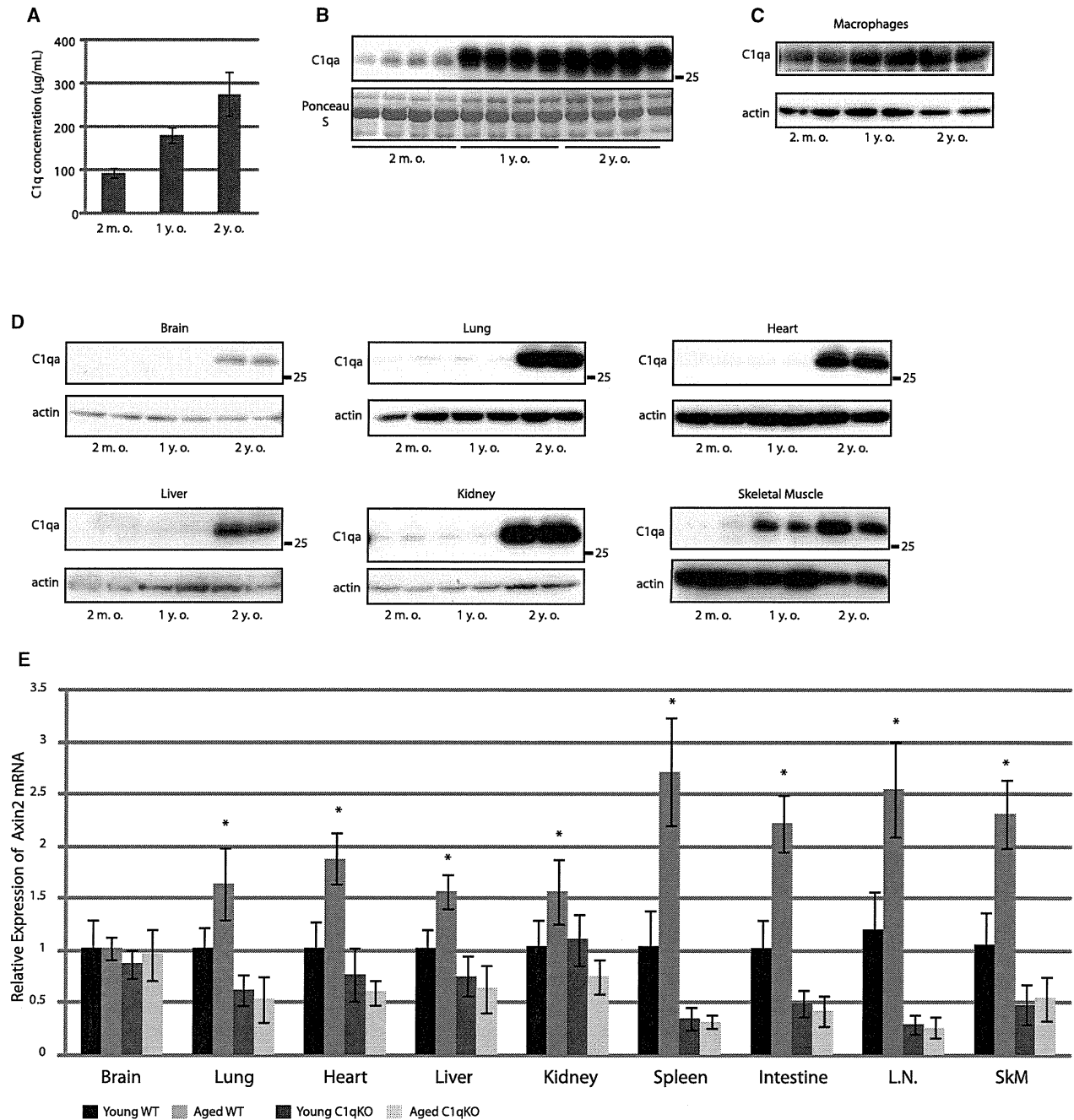


Figure 3. C1q Mediates Augmented Wnt Signaling Associated with Aging

(A and B) Serum C1q concentration of mice at different ages was assessed by ELISA (A) and western blot (B). Serum C1q concentration was increased with aging. Data in (A) are presented as mean \pm SD.

(C and D) Western blot analysis of C1q in peritoneal macrophages (C) and in various tissues (D) derived from wild-type mice at different ages. C1q expression in macrophages and skeletal muscle was increased at 1 year of age, whereas a robust increase in C1q expression in other tissues was observed at 2 years of age.

(E) Expression levels of *Axin2* mRNA in various tissues from young (3 months old) and aged (2 years old) wild-type (young, $n = 8$; aged, $n = 4$) and C1qa-deficient mice (young, $n = 8$; aged, $n = 3$). *Axin2* gene expression was increased with aging in multiple tissues of wild-type mice (WT), but not in those of C1qa-deficient mice (C1qKO). L.N., lymph node; SkM, skeletal muscle. Data are presented as mean \pm SD. * $p < 0.05$ compared with young wild-type mice.

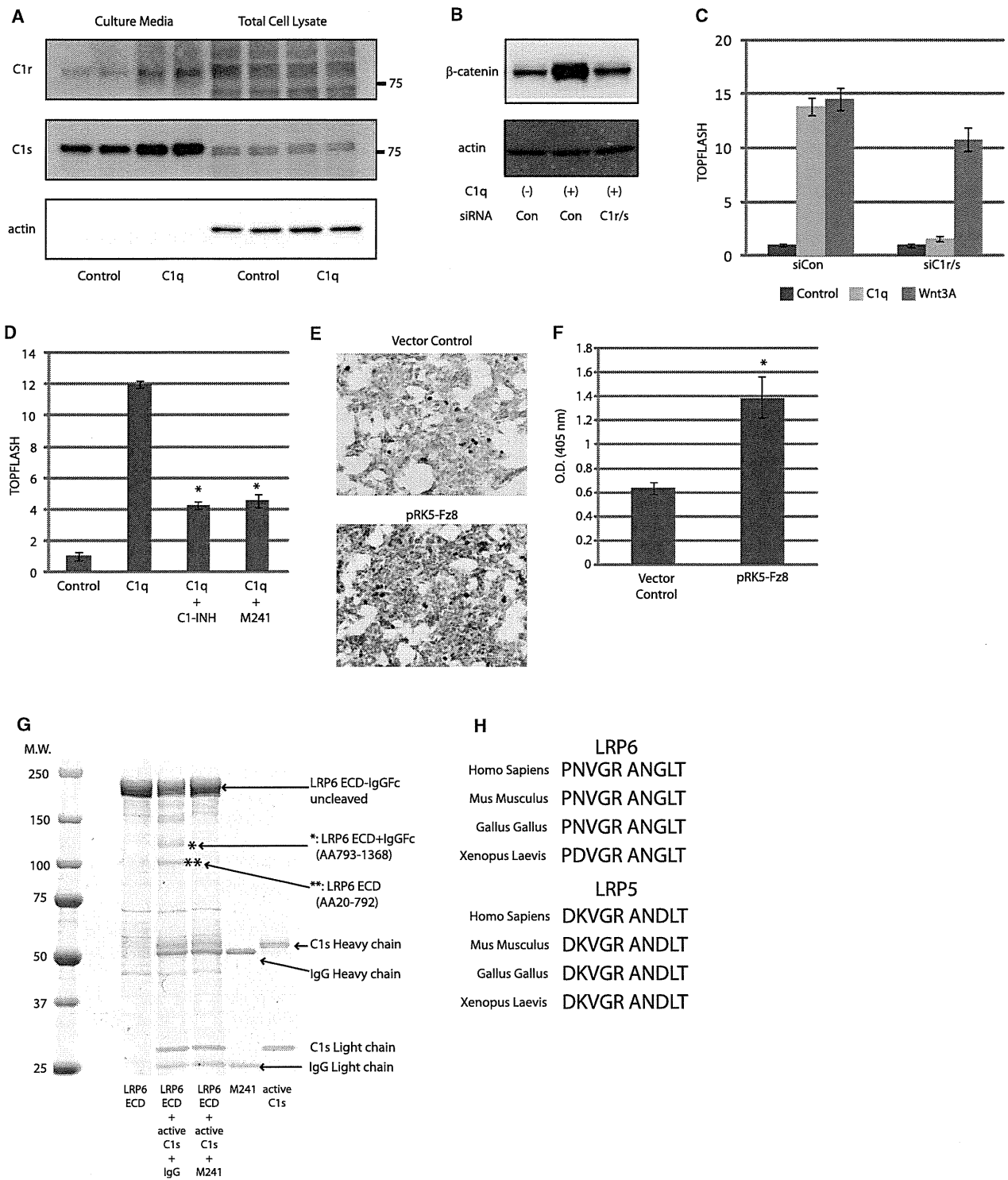


Figure 4. C1q-Induced Activation of Wnt Signaling Is Dependent on Protease Activity of C1s
 (A) HepG2 cells were cultured and stimulated with or without C1q (100 μg/ml) in a serum-free condition for 24 hr. Culture media and total cell lysate were analyzed by western blotting. Both C1r and C1s protein were observed in the culture media under serum-free condition.
 (B) β-catenin stabilization assay. HepG2 cells transfected with control siRNA (Con) responded to C1q (100 μg/ml), but those transfected with siRNAs against C1r and C1s (C1r/s) did not.

We also assessed whether C1q induces cleavage of endogenous LRP6 in HepG2 cells. C1q-induced activation of Wnt signaling was associated with the appearance of cleaved N-terminal fragment of LRP6 (~100 kDa) in culture media, which was detected by an antibody raised against extracellular portion of LRP6 (LRP6 ECD Ab), but not by an antibody against LRP6 intracellular domain (LRP6 ICD Ab) (Figure 5A). When cells were treated with C1q in the presence of a lysosomal inhibitor Chloroquine, LRP6 ICD Ab detected a protein compatible in size with the C-terminal cleaved fragment of LRP6 (~140 kDa) in the membrane/organelle fraction (Figure 5B). Notably, there was no apparent change in the expression levels of full-length LRP6 by C1q treatment, and this band was not observed in the absence of Chloroquine or when the cells were treated with Wnt3A (Figure 5B). Thus, a relatively small fraction of LRP6 is cleaved by C1s following C1q treatment, and the resultant C-terminal fragment of LRP6 produced by C1s cleavage appears to be subjected to lysosomal degradation.

We next tested whether serum induces cleavage of LRP6 in a C1q-dependent manner. HepG2 cells were transfected with N-terminally myc-tagged LRP6 and treated with serum. Western blot analysis following immunoprecipitation with anti-myc antibody revealed that the cleaved product of LRP6 was detected in the culture media following treatment with normal serum, but not with C1q-depleted serum (Figure 5C). The ability to cleave LRP6 was fully recovered after restoring C1q to C1q-depleted serum (Figure 5C). The N-terminal fragment of endogenous LRP6 was also detected in the serum from wild-type mice, but not in C1qa-deficient mice, and the concentration of LRP6 C-terminal cleaved fragment was increased by ~2-fold in aged mice compared with young mice (Figures 5D and 5E). These observations indicate that both serum-induced LRP6 cleavage *in vitro* and an age-dependent increase in LRP6 cleavage *in vivo* occur in a C1q-dependent manner.

To examine whether LRP6 cleavage by C1s is sufficient for Wnt signaling activation by C1q, we generated a LRP6 deletion mutant that lacks amino acids 21–792 (Del-LRP6). Transfection of Del-LRP6 increased Wnt signaling activity by 47-fold compared with wild-type LRP6 (WT-LRP6) (Figure 5F), suggesting that cleavage of LRP6 between Arg792 and Ala793 is sufficient for activation of canonical Wnt signaling. As phosphorylation of the intracellular region of LRP5/6 is a hallmark of LRP5/6 activation (Tamai et al., 2004; Zeng et al., 2005), we investigated the phosphorylation status of LRP6 after C1q stimulation. When the cells were treated with C1q together with Chloroquine for 3 hr, phosphorylation of cleaved LRP6

C-terminal fragment (~140 kDa) was detected (Figure S3A). Of note, we found that phosphorylation of full-length LRP6 was also increased following C1q treatment (Figure S3A). Moreover, transfected Del-LRP6 was strongly phosphorylated even in the absence of Wnt3A stimulation (Figure S3B) and induced the phosphorylation of simultaneously transfected full-length WT-LRP6 (Figure S3C). These results suggest that a relatively small amount of cleaved LRP5/6 fragment may amplify Wnt signaling by inducing the phosphorylation of uncleaved LRP5/6.

To test whether LRP6 cleavage by C1s is required for C1q-induced activation of Wnt signaling, we generated a C1s-resistant LRP6 mutant in which Arg792 and Ala793 were substituted to glycines (Mt-LRP6). Overexpression of WT-LRP6 or Mt-LRP6 induced an ~7-fold increase in TOPFLASH activity (Figure S3D). Although WT-LRP6-transfected cells and Mt-LRP6-transfected cells responded to Wnt3A treatment similarly, C1q treatment strongly enhanced TOPFLASH activity (~18-fold) in WT-LRP6-transfected cells but only marginally in Mt-LRP6-transfected cells (~1.7-fold) (Figures 5G, 5H, and S3D). This slight increase in C1q-induced TOPFLASH activity in Mt-LRP6-transfected cells presumably reflects the activation of Wnt signaling mediated by cleavage of endogenous LRP6. These results suggest the requirement of LRP6 cleavage in C1q-induced activation of Wnt signaling.

We next tested the requirement of C1r, C1s, LRP5/6, and Fz receptors in C1q-induced LRP6 cleavage and subsequent activation of Wnt signaling by siRNA-mediated knockdown of C1r, C1s, LRP5, and LRP6 (Figure S3E) or by overexpression of Shisa protein to reduce cell surface Fz receptors (Yamamoto et al., 2005; Zeng et al., 2008). The amount of C-terminal (LRP6 ICD) and N-terminal (LRP6 ECD) cleaved forms of LRP6 following C1q treatment was dramatically decreased by C1r/C1s knockdown, LRP5/6 knockdown, or Shisa overexpression (Figure 5I), which was associated with inhibition of C1q-induced β -catenin stabilization and TOPFLASH activation (Figure 5J). These results collectively suggest that C1q binding to Fz receptors results in the activation of C1r/C1s, which cleaves LRP5/6 and produces N-terminal truncated form of LRP5/6, leading to activation of canonical Wnt signaling (Figure 5K).

C1q Activates Wnt Signaling in Skeletal Muscle and Exhibits Differential Effects on Satellite Cells and Fibroblasts

Activation of Wnt signaling in skeletal muscle was shown to mediate a decrease in regenerative capacity and an increase in

(C) TOPFLASH assay. HEK293 cells transfected with control siRNA (siCon) responded to both C1q (100 μ g/ml) and Wnt3A (10 ng/ml), but those transfected with siRNAs against C1r and C1s (siC1r/s) responded to Wnt3A, but not to C1q. Data are presented as mean \pm SD.

(D) TOPFLASH assay. Activation of Wnt signaling by C1q (100 μ g/ml) was inhibited by an endogenous C1-inhibitor (C1-INH: 100 μ g/ml) or by a neutralizing antibody against C1s (M241: 100 μ g/ml). Proteins were fractionated by SDS-PAGE and visualized by Coomassie staining. C1s treatment of LRP6 ECD resulted in the appearance of two major bands (indicated by * and **). Amino acid sequencing revealed that * represented LRP6 ECD (amino acids 793–1368) + IgG/Fc, and ** represented LRP6 ECD (amino acids 20–792).

(E and F) C4 cleavage assay. C4b deposition on the cell surface was assessed by immunostaining (E) or ELISA (F). C4b deposition was increased after Fz8 overexpression. Data are presented as mean \pm SD. **p* < 0.05 versus control vector (*n* = 5).

(G) Coomassie staining of SDS-PAGE gel. LRP6 extracellular domain (ECD)-IgG/Fc fusion protein (4 μ g) was incubated with active-C1s (176 ng) with or without a neutralizing antibody against C1s (M241). Proteins were fractionated by SDS-PAGE and visualized by Coomassie staining. C1s treatment of LRP6 ECD resulted in the appearance of two major bands (indicated by * and **). Amino acid sequencing revealed that * represented LRP6 ECD (amino acids 793–1368) + IgG/Fc, and ** represented LRP6 ECD (amino acids 20–792).

(H) Amino acid sequence alignment of potential C1s cleavage site in the third β -propeller domain of LRP5 and LRP6. C1s cleavage site is predicted to be between arginine (R) and alanine (A). Cleavage site of C1s is highly conserved among species.

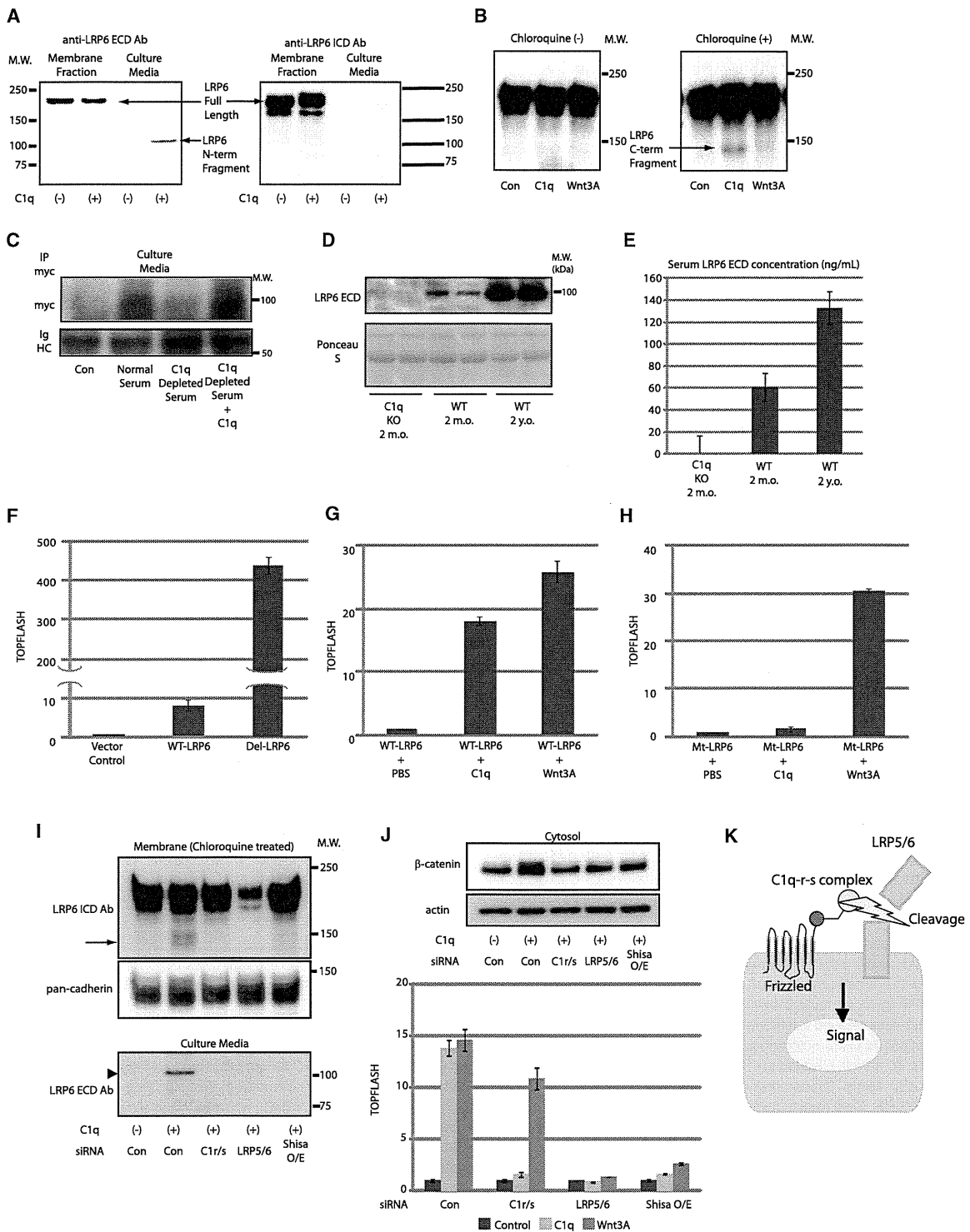


Figure 5. C1q Activates Wnt Signaling by Inducing C1s-Dependent Cleavage of the Extracellular Domain of LRP6
 (A) Western blot analysis of LRP6 fragment in the culture media from HepG2 cells treated with C1q (100 μg/ml). N-terminal cleaved fragment of endogenous LRP6 was detected in the culture media. ECD, extracellular domain; ICD, intracellular domain.
 (B) Western blot analysis of LRP6 in the membrane/organelle fraction of HepG2 cells treated with C1q (100 μg/ml) or Wnt3A (10 ng/ml). C-terminal cleaved fragment of LRP6 (~140 kDa) was detected by anti-LRP6 ICD Ab only in the cells treated with C1q plus lysosomal inhibitor Chloroquine (50 μM).

tissue fibrosis associated with aging (Brack et al., 2007). We examined the effects of C1q treatment on skeletal muscle satellite cells and fibroblasts because these cell types play important roles during skeletal muscle regeneration, the former being the source of new myocytes and the latter being responsible for fibrotic change of the regenerating tissue. We isolated satellite cells and fibroblasts from skeletal muscle of young mice and treated them with C1q or Wnt3A. Both treatments stabilized cytosolic β -catenin (Figure 6A) and increased *Axin2* gene expression (Figure S4A) in these cell types. Serum from aged mice also stabilized cytosolic β -catenin and increased *Axin2* gene expression more potently than serum from young mice, and this effect of serum from aged mice was inhibited by M241 (Figures 6B and S4B). These results suggest that C1q activates Wnt signaling both in satellite cells and fibroblasts and that C1q accounts for increased Wnt signaling activation by serum from aged mice in these cells.

We also tested whether C1q activates Wnt signaling in skeletal muscle in vivo using TOPGAL mice, which express β -galactosidase (β -gal) transgene under the control of Tcf/Lef-binding sites. For C1q application, we placed hydrogel containing C1q on the gastrocnemius muscle. Interestingly, C1q treatment alone did not activate Wnt signaling in skeletal muscle of young mice. However, 2 days after cryoinjury, Wnt signaling activity was slightly increased in injured skeletal muscle of control mice and was robustly enhanced in mice treated with C1q (Figures 6C and 6D). Real-time PCR analysis revealed that the expressions of *C1r* and *C1s*, but not *lrp5* or *lrp6*, were markedly upregulated after injury (Figure 6E), suggesting that induction of *C1r* and *C1s* contributes to the enhanced Wnt signaling activation by C1q in injured muscle.

We next examined the effect of C1q-induced activation of Wnt signaling on satellite cells and fibroblasts derived from skeletal muscle in vitro. We found that C1q and Wnt3A attenuated satellite cell proliferation, whereas they stimulated fibroblast proliferation (Figures 6F and 6G). C1q and Wnt3A also increased the collagen production/release from fibroblasts (Figure 6H). Likewise, serum from aged mice attenuated satellite cell proliferation, stimulated fibroblast proliferation, and increased collagen

production in fibroblasts, and these effects were abolished by M241 treatment (Figures 6I–6K). We also found that C1q treatment decreased the number of proliferating satellite cells and increased the number of proliferating fibroblasts in skeletal muscle in vivo (Figures 6L, 6M, S4C, and S4D). Taken together, reduced regenerative capacity associated with increased fibrosis in the skeletal muscle of aged organisms may be explained by differential effects of C1q-induced activation of Wnt signaling on satellite cells and fibroblasts.

C1q Mediates Impaired Skeletal Muscle Regeneration Associated with Aging

We then examined whether C1q mediates reduced regenerative capacity of skeletal muscle associated with aging. When the gastrocnemius muscle of young mice was cryoinjured and treated with C1q, canonical Wnt signaling was activated (Figure 7A). C1q treatment also strongly impaired regeneration and promoted fibrotic change in skeletal muscle (Figure 7B). Enhanced tissue fibrosis was also evidenced by increased expression of *Col3a1* gene and increased soluble collagen content in the regenerating muscle (Figures 7C and 7D). Activation of Wnt signaling and impairment of skeletal muscle regeneration after C1q treatment was also observed in C3-deficient mice (Figures 7A–7D), suggesting that the effect of C1q treatment on skeletal muscle regeneration is independent of the classical complement pathway activation.

We also cryoinjured the gastrocnemius muscle of aged wild-type and C1qa-deficient mice and placed the hydrogel containing either M241 or an anti-C5 antibody (BB5.1) that prevents the cleavage of C5. The former inhibits *C1s* and blocks both C1q-induced activation of Wnt signaling and the activation of the classical complement pathway, whereas the latter selectively blocks the classical complement pathway. *C1s* inhibition or *C1qa* gene disruption, but not the inhibition of complement activation, attenuated Wnt signaling activity in skeletal muscle and improved skeletal muscle regeneration with reduced tissue fibrosis following cryoinjury on aged mice (Figures 7E–7H). These results suggest that C1q-induced activation of Wnt signaling, but not C1q-triggered classical complement pathway

(C) Western blot analysis of the N-terminal cleaved form of LRP6 in culture media. N-terminal cleaved form of LRP6 was detected in culture media conditioned by cells treated with normal human serum, but not with C1q-depleted serum. Addition of purified C1q protein (100 μ g/ml) to C1q-depleted serum restored the activity to cleave LRP6. IgHC, immunoglobulin heavy chain.

(D and E) N-terminal cleaved fragment of LRP6 in the serum was analyzed by western blotting (D) and ELISA (E). In wild-type (WT) mice, the amount of cleaved form of endogenous LRP6 ectodomain was increased by 2-fold in serum from aged mice (2 years old: 130 ng/ml) compared with serum from young mice (2 months old: 60 ng/ml). Cleaved LRP6 was not detected in the serum from young C1qa-deficient mice. Data are presented as mean \pm SD.

(F–H) TOPFLASH assay. Overexpression of N-terminal truncated LRP6 (Del-LRP6) resulted in enhanced activation of Wnt signaling compared with wild-type LRP6 (WT-LRP6) (F). Cells transfected with WT-LRP6 responded to both C1q (100 μ g/ml) and Wnt3A (10 ng/ml) (G), whereas those transfected with *C1s*-resistant LRP6 (Mt-LRP6) responded to Wnt3A, but not to C1q (H). Data are presented as mean \pm SD.

(I) Western blot analysis of C-terminal LRP6 fragment in the membrane/organelle fraction and N-terminal LRP6 fragment in the culture media after treatment of HepG2 cells with C1q (100 μ g/ml). Both C-terminal and N-terminal LRP6/6 fragments were not detected in cells transfected with siRNAs against *C1r* and *C1s* (*C1r/s*), LRP5 and LRP6 (LRP5/6), or cells transfected with Shisa (Shisa O/E). An arrow indicates C-terminal LRP6 fragment, and an arrowhead indicates N-terminal LRP6 fragment.

(J) (Top) β -catenin stabilization assay. HepG2 cells transfected with control siRNA (Con) responded to C1q (100 μ g/ml), but those transfected with siRNAs against *C1r* and *C1s* (*C1r/s*), LRP5 and LRP6 (LRP5/6) or cells transfected with Shisa (Shisa O/E) did not. (Bottom) TOPFLASH assay. HEK293 cells transfected with control siRNA responded to both C1q (100 μ g/ml) and Wnt3A (10 ng/ml), whereas those transfected with siRNAs against *C1r* and *C1s* (*C1r/s*) responded to Wnt3A, but not to C1q. Data are presented as mean \pm SD.

(K) Schematic diagram of C1q-induced activation of Wnt signaling. Upon binding to Fz receptors, C1q activates *C1r/C1s*, which results in LRP5/6 cleavage and activation of Wnt signaling. See also Figure S3.

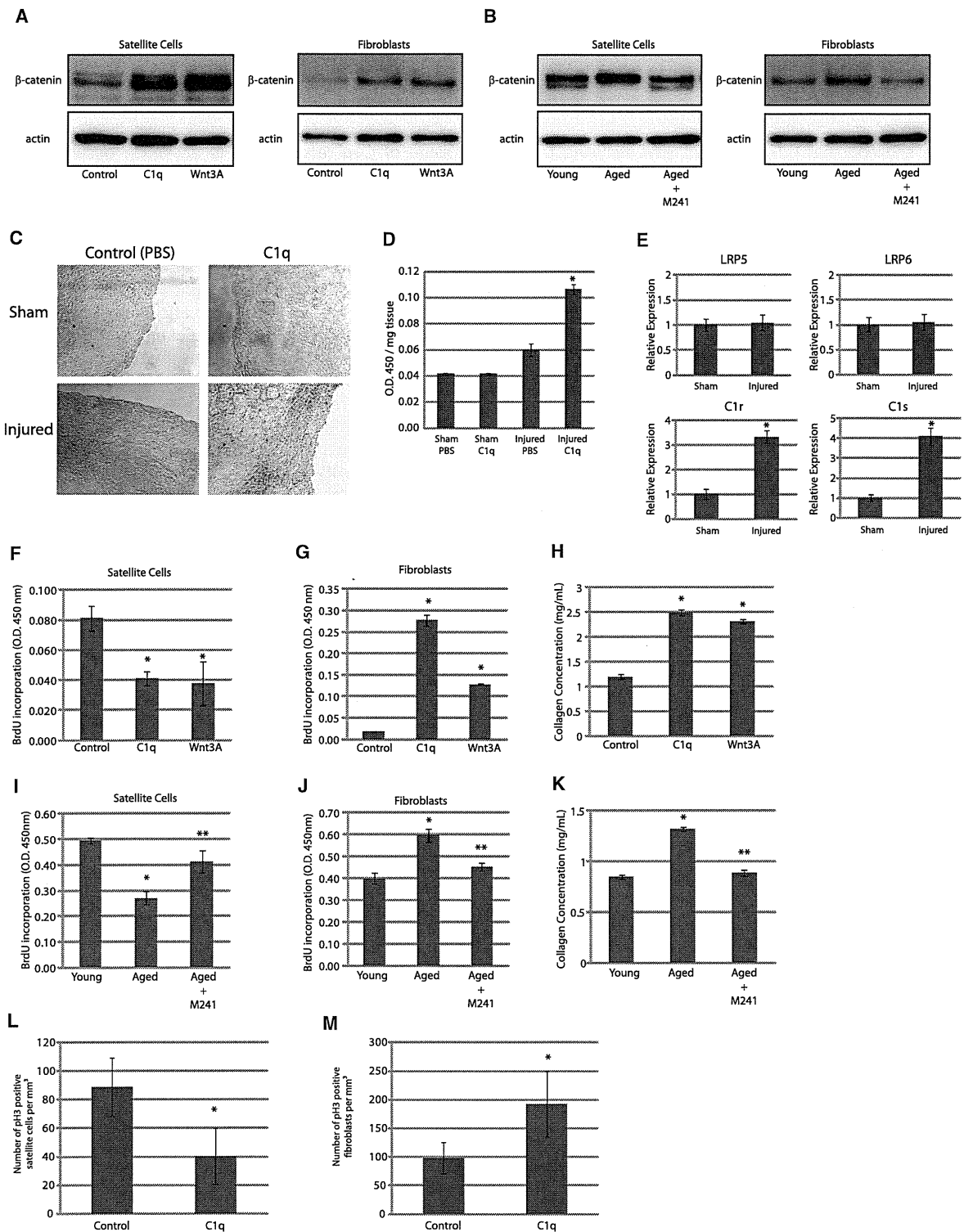


Figure 6. C1q Activates Wnt Signaling in Skeletal Muscle and Exhibits Differential Effects on Satellite Cells and Fibroblasts (A and B) β -catenin stabilization assay. Satellite cells and fibroblasts were stimulated with C1q (100 μ g/ml) or Wnt3A (10 ng/ml). Both C1q and Wnt3A activated Wnt signaling in these cells (A). Cells were also stimulated with serum derived from young (2 months old) or aged mice (2 years old). The extent of Wnt signaling activation by serum from aged mice was greater than that by serum from young mice, and activation of Wnt signaling by serum from aged mice was attenuated by M241.

activation, mediates reduced regenerative capacity in skeletal muscle associated with aging.

DISCUSSION

The results of our *in vitro* experiments provide compelling evidence showing that C1q activates Wnt signaling through C1s-dependent cleavage of the ectodomain of LRP6 (Figure 5K). The physiological relevance of C1q-induced activation of Wnt signaling *in vivo* is supported by the following observations. First, an aging-related increase in serum-induced activation of Wnt signaling correlated with an increase in the amount of serum C1q (Figures 1C, 2B, 3A, and 3B), and the concentration of C1q that was shown to activate canonical Wnt signaling in cell culture experiments (100 $\mu\text{g/ml}$) was within the physiological range of the serum concentration of C1q in humans and mice (Figure 3A) (Borquez et al., 1995; Yonemasu et al., 1978). Second, cleaved product of LRP6 was detected in the serum in wild-type mice, but not in C1qa-deficient mice, and its amount was increased with aging (Figures 5D and 5E). Third, the expression of *Axin2* gene was downregulated in various tissues of C1qa-deficient mice, but not of C3-deficient mice (Figure 2G). Fourth, enhanced Wnt signaling activation by serum and increased Wnt signaling in multiple tissues associated with aging were observed in wild-type, but not in C1qa-deficient mice (Figures 2B and 3E). These observations strongly suggest the physiological relevance of C1q-induced activation of Wnt signaling *in vivo*.

Although C1q and Wnt3A bind to Fz receptors with similar affinity (Figures 1I and S1E), EC_{50} value of C1q on TOPFLASH activity cells was much higher than that of Wnt3A (Figure 1M). In particular, the extent of Wnt signaling activation induced by 100 $\mu\text{g/ml}$ (200 nM) of C1q and 10 ng/ml (0.2 nM) of Wnt3A was comparable, as determined by *Axin2* mRNA induction (Figure 1L) and TOPFLASH reporter gene assay (Figure 4C), which indicates that 1,000 times more C1q molecules are required to

activate Wnt signaling to the same extent that Wnt3A does. These apparent discrepancies may be explained by the unique mode of Wnt signaling activation by C1q compared to that by classical Wnt proteins. Activation of Wnt signaling by C1q requires several rate-limiting steps, which include the activation of C1q, C1r, and C1s. For instance, whether conformational change of C1q required for its activation occurs at the cell surface may be affected by the local density of Fz receptors, analogous to the mechanism of C1q activation by immunoglobulins (Duncan and Winter, 1988; Schumaker et al., 1986). This notion is consistent with our data showing that increasing the amount of Fz receptors potentially decreased the EC_{50} value of C1q-induced activation of Wnt signaling (Figures 1M and 1N). Activation of C1r and C1s may be affected by their expression levels or by the local concentration of endogenous C1 inhibitor, which is also consistent with our observations that C1q-induced activation of Wnt signaling in skeletal muscle was observed only when the expressions of C1r and C1s were upregulated following injury (Figures 6C–6E) and that treatment with C1 inhibitor or knockdown of C1r/C1s reduced Wnt signaling activation by C1q (Figures 4B–4D and 5J). Thus, the extent of C1q-induced activation of Wnt signaling is highly context dependent and modulated not only by the concentration of C1q to which target cells are exposed, but also by many factors, including the expression levels of Fz receptors, LRP5/6 coreceptors, C1r, C1s, and C1 inhibitor in target cells.

LRP5/6 mutants lacking the extracellular domain have been reported to be a constitutively active form of canonical Wnt signaling (Liu et al., 2003; Mao et al., 2001). Our findings indicate that cleavage of extracellular N-terminal region of LRP5/6 by C1s occurs under physiological situations. Moreover, C1q treatment phosphorylated both cleaved and uncleaved LRP6, and overexpression of truncated LRP6 phosphorylated simultaneously overexpressed full-length LRP6 in the absence of ligand stimulation (Figures S3A–S3C), indicating that cleaved LRP5/6 fragment may amplify Wnt signaling by inducing the phosphorylation of

(C) X-gal staining of skeletal muscle after injury. Skeletal muscle of young (2 months old) TOPGAL mice was cryoinjured and treated with PBS or C1q (50 $\mu\text{g/ml}$). X-gal staining showed that β -gal activity was slightly increased 2 days after cryoinjury, which was enhanced by C1q.

(D) Quantitative analysis of β -gal activity. TOPGAL mice were treated as in (C), and tissue β -gal activity was measured and corrected with tissue weight. Data are presented as mean \pm SD. * $p < 0.01$ versus sham-operated mice treated with PBS ($n = 10$).

(E) Real-time PCR analysis. Mice were treated as in (C), and the expressions of *lrp5*, *lrp6*, *C1r*, and *C1s* were analyzed by real-time PCR. Data are presented as mean \pm SD. * $p < 0.01$ versus sham-operated mice ($n = 6$).

(F and G) BrdU incorporation assay in satellite cells (F) and fibroblasts (G). Satellite cells and fibroblasts were stimulated with C1q (100 $\mu\text{g/ml}$) or Wnt3A (10 ng/ml) for 24 hr. BrdU incorporation during the last 12 hr (satellite cells) or 4 hr (fibroblasts) was assayed by ELISA. C1q and Wnt3A inhibited satellite cell proliferation and stimulated fibroblast proliferation. Data are presented as mean \pm SD. * $p < 0.01$ versus control ($n = 4$).

(H) Collagen concentration in the culture media. After stimulation with C1q (100 $\mu\text{g/ml}$) or Wnt3A (10 ng/ml) for 24 hr, medium was changed to serum-free medium, and soluble collagen released to the medium was quantified 6 hr later. C1q and Wnt3A increased collagen production in fibroblasts. Data are presented as mean \pm SD. * $p < 0.01$ compared with control ($n = 4$).

(I and J) BrdU incorporation assay in satellite cells (I) and fibroblasts (J). Satellite cells and fibroblasts were cultured and stimulated with serum (5%) for 24 hr. BrdU incorporation was assayed as in (F) and (G). Serum from aged mice reduced satellite cell proliferation and stimulated fibroblast proliferation, which was attenuated by M241. Data are presented as mean \pm SD. * $p < 0.01$ versus serum from young mice. ** $p < 0.01$ versus serum from aged mice ($n = 4$).

(K) Collagen concentration in the culture media. After stimulation with serum for 24 hr, soluble collagen in the medium was assayed as in (H). Serum from aged mice increased collagen production in fibroblasts, which was attenuated by M241 treatment. * $p < 0.01$ versus serum from young mice. Data are presented as mean \pm SD. ** $p < 0.01$ versus serum from aged mice ($n = 4$).

(L and M) Number of proliferating satellite cells (L) and fibroblasts (M) in cryoinjured skeletal muscle of young mice (2 months old) *in vivo*. Sections were immunostained with M-cadherin (a satellite cell marker), Vimentin (a fibroblast marker), and phospho-histone H3 (pH3) (a mitotic marker). Proliferating satellite cells and fibroblasts were identified as M-cadherin/pH3 double-positive cells and Vimentin/pH3 double-positive cells, respectively. C1q treatment reduced satellite cell proliferation and stimulated fibroblast proliferation in cryoinjured skeletal muscle. Data are presented as mean \pm SD. * $p < 0.05$ versus control ($n = 5$). See also Figure S4.

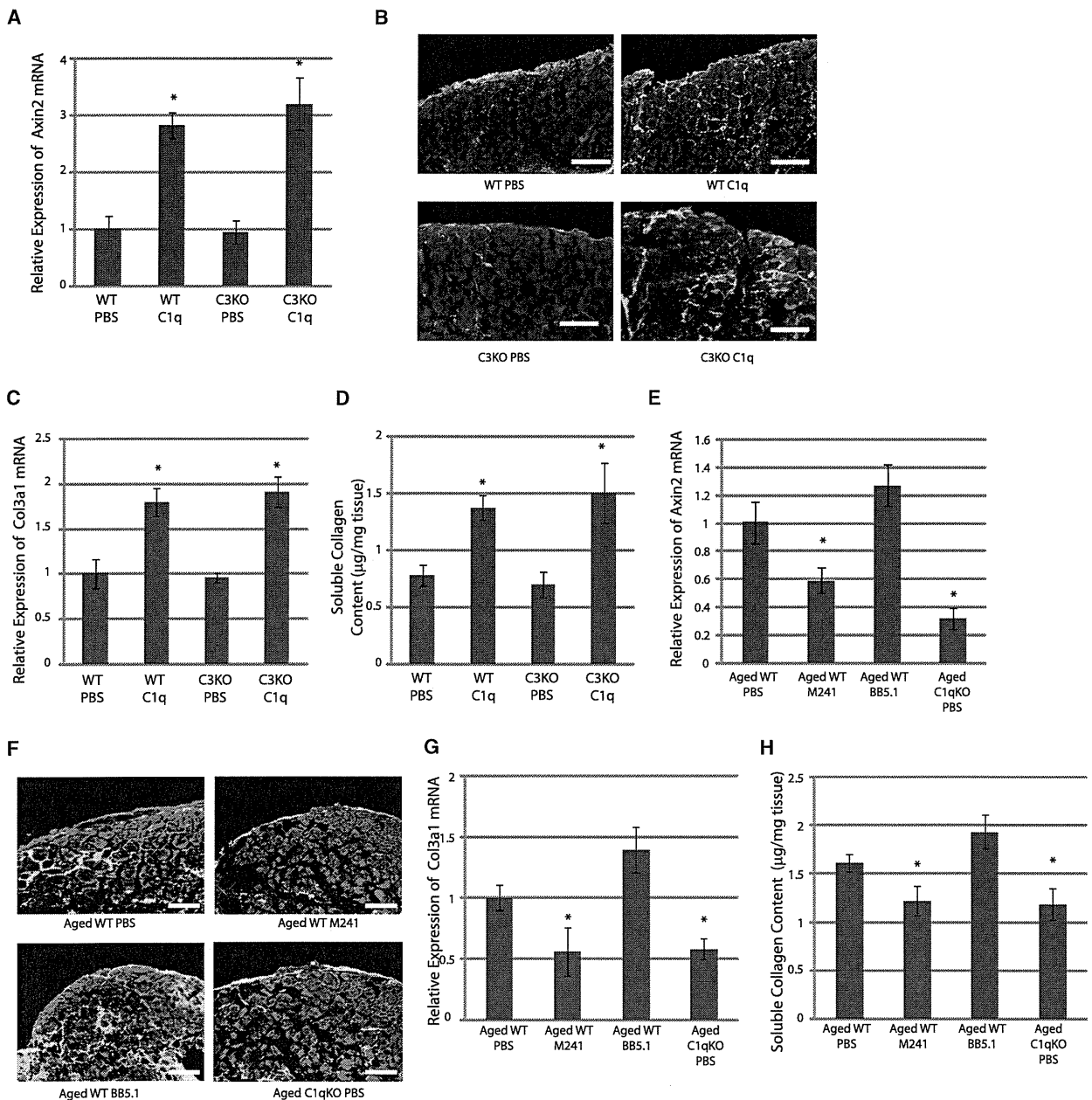


Figure 7. C1q Mediates Reduced Regenerative Capacity of Skeletal Muscle Associated with Aging

(A) *Axin2* mRNA expression. Skeletal muscle of young (2 months old) wild-type (WT) and C3-deficient (C3KO) mice was cryoinjured and treated with PBS or C1q (50 μ g/ml). RNA was extracted 3 days later. C1q treatment increased *Axin2* gene expression in injured skeletal muscle of both wild-type and C3-deficient mice. Data are presented as mean \pm SD. * p < 0.01 versus PBS (n = 4).

(B) Immunostaining of skeletal muscle after cryoinjury. Tissue samples were harvested 5 days after injury and immunostained with embryonic myosin heavy-chain (Red) and type I/III Collagen (green). Four wild-type mice (eight samples) and three C3-deficient mice (six samples) were used for each group, and representative figures are shown. C1q treatment impaired muscle regeneration and increased fibrosis in both wild-type and C3-deficient mice. Scale bar, 150 μ m.

(C) Expression of *Col3a1* gene. RNA was harvested 3 days after injury. C1q treatment increased *Col3a1* expression in injured skeletal muscle of both wild-type and C3-deficient mice. Data are presented as mean \pm SD. * p < 0.01 versus PBS (n = 4).

(D) Soluble collagen content in skeletal muscle. Samples were harvested 5 days after injury. C1q treatment increased soluble collagen content in skeletal muscle after cryoinjury of both wild-type and C3-deficient mice. Data are presented as mean \pm SD. * p < 0.01 versus PBS (n = 4).

(E) *Axin2* mRNA expression. Skeletal muscle of aged (2 years old) wild-type (WT) mice or aged C1qa-deficient mice (C1qKO) was cryoinjured and treated with M241 or BB5.1 (500 μ g/ml each). RNA was extracted 3 days after cryoinjury. The expression of *Axin2* was suppressed by M241 treatment or in C1qa-deficient mice, but not by BB5.1 treatment. Data are presented as mean \pm SD. * p < 0.01 versus aged WT PBS (n = 4).

uncleaved LRP5/6. Although the precise mechanism by which full-length LRP5/6 is phosphorylated in the presence of cleaved form of LRP5/6 is currently unknown, these observations may, in part, explain the reason why cleavage of a small fraction of LRP5/6 by C1q treatment leads to activation of Wnt signaling to the comparable level induced by Wnt3A.

In addition to its role in innate immunity, C1q is implicated in the pathogenesis of various diseases, including autoimmunity and neurodegenerative diseases (Nayak et al., 2010). C1q deficiency in humans is tightly associated with the development of systemic lupus erythematosus (SLE) (Pickering et al., 2000), and it has been reported that Wnt/ β -catenin signaling plays a role in the immune system by regulating T cell development and dendritic cell maturation (Manicassamy et al., 2010; Staal et al., 2008; Xu et al., 2003). It would be interesting to test whether downregulation of Wnt signaling activity in lymphocytes plays a role in the development of autoimmunity. In the central nervous system, complement system can be both protective and deleterious because it works to eliminate toxic proteins, whereas its sustained activation induces the production of cytokines or oxidative products from microglia (Bonifati and Kishore, 2007). C1q also mediates synapse elimination during development and is reactivated in the retina of mice with glaucoma (Stevens et al., 2007). Intriguingly, activation of Wnt signaling in the brain has also been reported to be both protective and deleterious (Boonen et al., 2009), and Wnt signaling has been shown to exert both positive and negative effects on synapse formation (Klassen and Shen, 2007; Packard et al., 2002). It remains elusive whether increased activation of canonical Wnt signaling by C1q contributes to aging-associated neurological disorders.

In summary, we have shown that complement C1q is an activator of canonical Wnt signaling and that activation of Wnt signaling by C1q mediates impaired regenerative capacity of skeletal muscle in aged animals. These findings suggest that C1q-induced activation of Wnt signaling plays an important role in other aging-related phenotypes as well as in the pathogenesis of various diseases that are related to augmented Wnt signaling. Likewise, impaired function of C1q may play a pathogenic role in the disease states associated with reduced Wnt signaling. Modulation of C1q-dependent activation of Wnt signaling may provide a therapeutic strategy for diseases linked to dysregulated Wnt signaling.

EXPERIMENTAL PROCEDURES

Cell Culture

HEK293, NIH 3T3, and HepG2 cells were cultured in DMEM containing 10% fetal bovine serum. Satellite cells in skeletal muscle were isolated as described (Brack et al., 2007). Fibroblasts in skeletal muscle were prepared by repeated digestion of skeletal muscle by trypsin.

TOPFLASH Assay

TOPFLASH assay was performed using a HEK293 cell line stably transfected with a luciferase reporter gene under the control of eight Tcf/Lef-binding sites (Super 8XTOPFLASH) (Veeman et al., 2003). Twenty-four hours after passage, cells were serum starved for 3 hr before stimulation. Luciferase assay was performed 24 hr after stimulation. Luciferase activity was determined using One-Glo (Promega), as described (Naito et al., 2006). Experiments were performed in triplicate for at least three different samples. Results are shown as the fold induction of the luciferase activity relative to the control.

β -Catenin Stabilization Assay

HEK293 or HepG2 cells were used for β -catenin stabilization assay. Twenty-four hours after passage, cells were serum starved for 24 hr before stimulation. At 1 hr after stimulation, cytosolic fraction was obtained by ultracentrifugation.

RNA Analysis

Relative levels of gene expression were quantified by the comparative Ct method using Universal Probe Library (UPL) (Roche) and Light Cycler TaqMan Master kit (Roche).

Protein Analysis

Total cell lysate was collected in lysis buffer containing 1% Triton X-100. Cytosolic and membrane/organelle fraction was obtained by differential centrifugation. Culture medium was concentrated using Amicon Ultra (Millipore) or immunoprecipitated with anti-myc antibody.

Binding Assays

C1q/Wnt3A was labeled with succinimidyl alkyne (Invitrogen), and various concentrations of labeled C1q/Wnt3A were mixed with 500 fmol (~21.65 ng) of Fz8/Fc in a volume of 100 μ l (5 nM). C1q/Wnt3A that bound to Fz8/Fc was coprecipitated with protein G, eluted, quantified by ELISA using biotinazide and HRP-streptavidin, and shown as the molar that binds specifically to 1 mg of Fz8/Fc. Unbound C1q/Wnt3A was collected and also quantified by ELISA.

Cell Proliferation Assay

Proliferation of cultured satellite cells and fibroblasts derived from skeletal muscle was assayed using Cell Proliferation ELISA, BrdU (Colorimetric) (Roche). Different durations of BrdU labeling time between satellite cells and fibroblasts are due to their difference in proliferative capacity.

Soluble Collagen Assay

Collagen content in culture media was assayed using Sircoll Collagen Assay (Bioroll). Tissue collagen content was assessed in the same manner after extraction of salt-soluble collagens using extraction buffer (50 mM Tris and 1.0 M NaCl plus protease inhibitors).

Animals

All protocols were approved by the Institutional Animal Care and Use Committee of Chiba University and Osaka University. TOPGAL mice were from Jackson laboratory. C1qa-deficient mice (Botto et al., 1998) and C3-deficient mice (Wessels et al., 1995) were previously described. Mice backcrossed to C57BL/6 background were used.

Statistical Analysis

Data are expressed as mean \pm SD. The significance of differences among means was evaluated using analysis of variance (ANOVA), followed by

(F) Immunostaining of skeletal muscle after cryoinjury. Tissue samples were harvested 5 days after injury and immunostained as in (B). Three wild-type mice (six samples) and two C1qa-deficient mice (four samples) were used, and representative figures are shown. Impaired skeletal muscle regeneration in aged mice was restored by M241 treatment, but not by BB5.1 treatment, and was not observed in C1qa-deficient mice. Scale bar, 150 μ m.

(G) Expression of *Col3a1* gene. RNA was extracted 3 days after cryoinjury. The expression of *Col3a1* gene was reduced by M241 treatment or in C1qa-deficient mice, but not by BB5.1 treatment. Data are presented as mean \pm SD. * $p < 0.01$ versus aged WT PBS ($n = 4$).

(H) Soluble collagen content in skeletal muscle. Samples were harvested 5 days after cryoinjury. Soluble collagen content was attenuated by M241 treatment or in C1qa-deficient mice, but not by BB5.1 treatment. Data are presented as mean \pm SD. * $p < 0.01$ versus aged WT PBS ($n = 6$).

Mann-Whitney's U test or Fisher's PLSD test for comparisons. Significant differences were defined as $p < 0.05$.

SUPPLEMENTAL INFORMATION

Supplemental Information includes Extended Experimental Procedures and four figures and can be found with this article online at doi:10.1016/j.cell.2012.03.047.

ACKNOWLEDGMENTS

We thank X. He, R.T. Moon, C. Niehrs, and S. Aizawa for plasmids and A. Furuyama, M. Iiyama, M. Ikeda, M. Kikuchi, M. Naito, Y. Ohtsuki, and I. Sakamoto for technical support. This work was supported by grants from the Ministry of Education, Culture, Sports, Science and Technology (MEXT); the Ministry of Health, Labour, and Welfare; and Japan Science and Technology Agency (to I.K.). This work was also supported by Grant-in-Aid for Young Scientists (A), Grant-in-Aid for JSPS Fellows, Research Grant from the Japan Prize Foundation, and the Japan Foundation for Applied Enzymology (to A.T.N.).

Received: March 8, 2010

Revised: November 13, 2010

Accepted: March 28, 2012

Published: June 7, 2012

REFERENCES

- Ahn, V.E., Chu, M.L., Choi, H.J., Tran, D., Abo, A., and Weis, W.I. (2011). Structural basis of Wnt signaling inhibition by Dickkopf binding to LRP5/6. *Dev. Cell* **21**, 862–873.
- Angers, S., and Moon, R.T. (2009). Proximal events in Wnt signal transduction. *Nat. Rev. Mol. Cell Biol.* **10**, 468–477.
- Blanpain, C., Horsley, V., and Fuchs, E. (2007). Epithelial stem cells: turning over new leaves. *Cell* **128**, 445–458.
- Bonifati, D.M., and Kishore, U. (2007). Role of complement in neurodegeneration and neuroinflammation. *Mol. Immunol.* **44**, 999–1010.
- Boonen, R.A., van Tijn, P., and Zivkovic, D. (2009). Wnt signaling in Alzheimer's disease: up or down, that is the question. *Ageing Res. Rev.* **8**, 71–82.
- Borquez, L., Oliván, V., and Iguaz, F. (1995). Development and validation of an automated particle-enhanced nephelometric immunoassay method for the measurement of human plasma C1q. *J. Clin. Lab. Anal.* **9**, 302–307.
- Botto, M., Dell'Agnola, C., Bygrave, A.E., Thompson, E.M., Cook, H.T., Petry, F., Loos, M., Pandolfi, P.P., and Walport, M.J. (1998). Homozygous C1q deficiency causes glomerulonephritis associated with multiple apoptotic bodies. *Nat. Genet.* **19**, 56–59.
- Brack, A.S., Conboy, M.J., Roy, S., Lee, M., Kuo, C.J., Keller, C., and Rando, T.A. (2007). Increased Wnt signaling during aging alters muscle stem cell fate and increases fibrosis. *Science* **317**, 807–810.
- Chen, S., Bubeck, D., MacDonald, B.T., Liang, W.X., Mao, J.H., Malinauskas, T., Llorca, O., Aricescu, A.R., Siebold, C., He, X., and Jones, E.Y. (2011). Structural and functional studies of LRP6 ectodomain reveal a platform for Wnt signaling. *Dev. Cell* **21**, 848–861.
- Clevers, H. (2006). Wnt/beta-catenin signaling in development and disease. *Cell* **127**, 469–480.
- Duncan, A.R., and Winter, G. (1988). The binding site for C1q on IgG. *Nature* **332**, 738–740.
- Eriksson, H., and Nissen, M.H. (1990). Proteolysis of the heavy chain of major histocompatibility complex class I antigens by complement component C1s. *Biochim. Biophys. Acta* **1037**, 209–215.
- Kang, Y.S., Do, Y., Lee, H.K., Park, S.H., Cheong, C., Lynch, R.M., Loeffler, J.M., Steinman, R.M., and Park, C.G. (2006). A dominant complement fixation pathway for pneumococcal polysaccharides initiated by SIGN-R1 interacting with C1q. *Cell* **125**, 47–58.
- Kikuchi, A., Yamamoto, H., and Kishida, S. (2007). Multiplicity of the interactions of Wnt proteins and their receptors. *Cell. Signal.* **19**, 659–671.
- Klassen, M.P., and Shen, K. (2007). Wnt signaling positions neuromuscular connectivity by inhibiting synapse formation in *C. elegans*. *Cell* **130**, 704–716.
- Liu, G., Bafico, A., Harris, V.K., and Aaronson, S.A. (2003). A novel mechanism for Wnt activation of canonical signaling through the LRP6 receptor. *Mol. Cell Biol.* **23**, 5825–5835.
- Liu, H., Fergusson, M.M., Castilho, R.M., Liu, J., Cao, L., Chen, J., Malide, D., Rovira, I.I., Schimel, D., Kuo, C.J., et al. (2007). Augmented Wnt signaling in a mammalian model of accelerated aging. *Science* **317**, 803–806.
- Logan, C.Y., and Nusse, R. (2004). The Wnt signaling pathway in development and disease. *Annu. Rev. Cell Dev. Biol.* **20**, 781–810.
- MacDonald, B.T., Tamai, K., and He, X. (2009). Wnt/beta-catenin signaling: components, mechanisms, and diseases. *Dev. Cell* **17**, 9–26.
- Manicassamy, S., Reizis, B., Ravindran, R., Nakaya, H., Salazar-Gonzalez, R.M., Wang, Y.C., and Pulendran, B. (2010). Activation of beta-catenin in dendritic cells regulates immunity versus tolerance in the intestine. *Science* **329**, 849–853.
- Mao, B., Wu, W., Li, Y., Hoppe, D., Stannek, P., Glinka, A., and Niehrs, C. (2001). LDL-receptor-related protein 6 is a receptor for Dickkopf proteins. *Nature* **411**, 321–325.
- Matsumoto, M., and Nagaki, K. (1986). Functional analysis of activated C1s, a subcomponent of the first component of human complement, by monoclonal antibodies. *J. Immunol.* **137**, 2907–2912.
- Naito, A.T., Shiojima, I., Akazawa, H., Hidaka, K., Morisaki, T., Kikuchi, A., and Komuro, I. (2006). Developmental stage-specific biphasic roles of Wnt/beta-catenin signaling in cardiomyogenesis and hematopoiesis. *Proc. Natl. Acad. Sci. USA* **103**, 19812–19817.
- Nayak, A., Fertuga, J., Tzolaki, A.G., and Kishore, U. (2010). The non-classical functions of the classical complement pathway recognition subcomponent C1q. *Immunol. Lett.* **131**, 139–150.
- Packard, M., Koo, E.S., Gorczyca, M., Sharpe, J., Cumberledge, S., and Budnik, V. (2002). The *Drosophila* Wnt, wingless, provides an essential signal for pre- and postsynaptic differentiation. *Cell* **111**, 319–330.
- Petry, F., Botto, M., Holtappels, R., Walport, M.J., and Loos, M. (2001). Reconstitution of the complement function in C1q-deficient (C1q^{-/-}) mice with wild-type bone marrow cells. *J. Immunol.* **167**, 4033–4037.
- Pickering, M.C., Botto, M., Taylor, P.R., Lachmann, P.J., and Walport, M.J. (2000). Systemic lupus erythematosus, complement deficiency, and apoptosis. *Adv. Immunol.* **76**, 227–324.
- Schumaker, V.N., Hanson, D.C., Kilchherr, E., Phillips, M.L., and Poon, P.H. (1986). A molecular mechanism for the activation of the first component of complement by immune complexes. *Mol. Immunol.* **23**, 557–565.
- Staal, F.J., Luis, T.C., and Tiemessen, M.M. (2008). WNT signalling in the immune system: WNT is spreading its wings. *Nat. Rev. Immunol.* **8**, 581–593.
- Stevens, B., Allen, N.J., Vazquez, L.E., Howell, G.R., Christopherson, K.S., Nouri, N., Micheva, K.D., Mehalow, A.K., Huberman, A.D., Stafford, B., et al. (2007). The classical complement cascade mediates CNS synapse elimination. *Cell* **131**, 1164–1178.
- Tamai, K., Zeng, X., Liu, C., Zhang, X., Harada, Y., Chang, Z., and He, X. (2004). A mechanism for Wnt coreceptor activation. *Mol. Cell* **13**, 149–156.
- Veeman, M.T., Slusarski, D.C., Kaykas, A., Louie, S.H., and Moon, R.T. (2003). Zebrafish prickles, a modulator of noncanonical Wnt/Fz signaling, regulates gastrulation movements. *Curr. Biol.* **13**, 680–685.
- Walport, M.J. (2001). Complement. First of two parts. *N. Engl. J. Med.* **344**, 1058–1066.
- Wessels, M.R., Butko, P., Ma, M., Warren, H.B., Lage, A.L., and Carroll, M.C. (1995). Studies of group B streptococcal infection in mice deficient in complement component C3 or C4 demonstrate an essential role for complement in both innate and acquired immunity. *Proc. Natl. Acad. Sci. USA* **92**, 11490–11494.
- White, B.D., Nguyen, N.K., and Moon, R.T. (2007). Wnt signaling: it gets more humorous with age. *Curr. Biol.* **17**, R923–R925.

Xu, Y., Banerjee, D., Huelsken, J., Birchmeier, W., and Sen, J.M. (2003). Deletion of beta-catenin impairs T cell development. *Nat. Immunol.* *4*, 1177–1182.

Yamamoto, A., Nagano, T., Takehara, S., Hibi, M., and Aizawa, S. (2005). Shisa promotes head formation through the inhibition of receptor protein maturation for the caudalizing factors, Wnt and FGF. *Cell* *120*, 223–235.

Yonemasu, K., Kitajima, H., Tanabe, S., Ochi, T., and Shinkai, H. (1978). Effect of age on C1q and C3 levels in human serum and their presence in colostrum. *Immunology* *35*, 523–530.

Zeng, X., Tamai, K., Doble, B., Li, S., Huang, H., Habas, R., Okamura, H., Woodgett, J., and He, X. (2005). A dual-kinase mechanism for Wnt co-receptor phosphorylation and activation. *Nature* *438*, 873–877.

Zeng, X., Huang, H., Tamai, K., Zhang, X., Harada, Y., Yokota, C., Almeida, K., Wang, J., Doble, B., Woodgett, J., et al. (2008). Initiation of Wnt signaling: control of Wnt coreceptor Lrp6 phosphorylation/activation via frizzled, dishevelled and axin functions. *Development* *135*, 367–375.